

**Development of a Dynamic Biomechanical Model for Load Carriage:  
Phase IV Part A&B:**

**Development of a Dynamic Biomechanical Model Version 2 of  
Human Load Carriage**

by:

S.A. Reid, J.T. Bryant, J.M. Stevenson, and M. Abdoli

Ergonomics Research Group  
Queen's University  
Kingston, Ontario, Canada  
K7L 3N6

Project Manager:

J. M. Stevenson (613) 533-6288

PWGSC Contract No. W7711-0-7632-07

on behalf of

DEPARTMENT OF NATIONAL DEFENCE

as represented by

Defence Research and Development Canada -Toronto  
1133 Sheppard Avenue West  
North York, Ontario, Canada  
M3M 3B9

DRDC Scientific Authority:

Mr Walter Dyck  
(613) 996-9347

August 2005

The scientific or technical validity of this Contract Report is entirely the responsibility of the contractor and the contents do not necessarily have the approval or endorsement of Defence R&D Canada

© Her Majesty the Queen as represented by the Minister of National Defence, 2005

© Sa Majesté la Reine, représentée par le ministre de la Défense nationale, 2005



## Abstract

The purpose of this DRDC dynamic biomechanical model research program is to improve the understanding of human load carriage capabilities and to understand the effects of load carriage design features on human health and mobility. This research is directed at creating a method of determining several of the biomechanical factors to be used as inputs to the Load Conditions Limit model as described in DRDC report # W7711—0-7632-01 entitled “Proposed Long Range Plan for a Research and Development Program of Dynamic Load Carriage Modeling”

In the current study, a 3D solid model was split into an upper and lower torso coupled with a rigid join located at the location of the spine at the L3/L2 height. Acceleration histories of subjects wearing packs were previously recorded during human trials (Morin et al, 2002). Acceleration of a person was numerically integrated and used to drive the motion of the Dynamic Biomechanical Model (DBM) torso. Torso accelerations for a wide range of activities were recorded and can be used to drive these models, creating an excellent data base for many human and pack motions for current and future modeling of human motions. This technique of capturing and generating motions is applicable to many situations where an envelope of human motion and body accelerations needs to be tested to ensure equipment does not cause excessive dynamic loading on the soldier.

Piecewise linear dynamic, static and creep material response models were developed for typical backpack materials. In addition, a piecewise linear model of the dynamic stress-strain response for the Cloth the Soldier shoulder strap assembly was developed.

The model estimates reaction forces and moments on the lumbar spine and the total shoulder reaction force. The model also calculates the distribution of force to the upper and lower torso and the total contact force.

Work is proceeding on incorporating a skin layer and creating the ability to examine interaction details at the equipment - skin interface. The final goal is to estimate injury risk potential across a range of activities and loads.

## Résumé

Le programme de recherche sur la modélisation biomécanique dynamique menée par RDDC a pour objectif d'améliorer la compréhension des capacités humaines de transport de charge et de comprendre les effets des caractéristiques de conception de systèmes de transport de charge sur la santé et la mobilité humaines. La présente étude vise à élaborer une méthode pour déterminer plusieurs facteurs biomécaniques qui pourraient être utilisés comme paramètres d'entrée dans le modèle de limite de charge décrit dans le rapport de RDDC n° W7711—0-7632-01 intitulé « Plan à long terme proposé pour le programme de recherche et de développement d'un modèle dynamique de transport de charge ».

Aux fins de la présente étude, un modèle volumique de torse a été scindé en un torse supérieur et en un torse inférieur reliés par un joint rigide à la hauteur des vertèbres L3/L2 de la colonne vertébrale. Durant des essais antérieurs effectués sur des humains, on a consigné l'historique des accélérations de sujets équipés de sac à dos (Morin et al, 2002). L'accélération d'une personne a été intégrée numériquement et a été utilisée pour réaliser le mouvement du torse pour le modèle biomécanique dynamique (DBM). Les valeurs d'accélération du torse ont été consignées pour un grand nombre d'activités et elles peuvent servir à alimenter les modèles pour ces activités et ainsi créer une excellente base de données contenant bon nombre de mouvements d'humains et de sacs en vue de la modélisation en cours et future des mouvements humains. Cette technique de saisie et de production de mouvements s'applique à un grand nombre de situations où il faut tester une enveloppe de mouvements humains et d'accélérations corporelles afin de s'assurer que l'équipement ne constitue pas une charge dynamique excessive pour le soldat.

On a élaboré des modèles linéaires par morceaux de la réponse dynamique, de la réponse statique et du fluage pour les matériaux types utilisés dans la fabrication des sacs à dos. De plus, un modèle linéaire par morceaux de la réponse dynamique à l'effort-déformation de l'ensemble de sangles d'épaules du programme Habillez le soldat a été développé.

Le modèle permet d'évaluer les forces de réaction et les moments sur la colonne lombaire et la force de réaction globale des épaules. Il permet également de calculer la répartition de la force entre le torse supérieur et le torse inférieur et la force totale de contact.

Les travaux sont en cours en vue de l'intégration d'une couche de peau, ce qui permettrait d'examiner en détail l'interaction au niveau de l'interface équipement-peau. Le but consiste à évaluer les risques de blessures pour une gamme d'activités et de charges.

## Executive Summary

The overall purpose of the DRDC dynamic biomechanical model (DBM) research program is to improve the understanding of human load carriage capabilities and to understand the effects of load carriage design features on human health and mobility. In addition, this research is directed at creating a method of determining several of the biomechanical factors to be used as inputs to the Load Conditions Limit model as described in DRDC report # W7711—0-7632-01 entitled “Proposed Long Range Plan for a Research and Development Program of Dynamic Load Carriage Modeling.”

Previous phases of dynamic biomechanical modeling research have led to an understanding of modeling that treats object-person interfaces as an interface contact pressure problem. In solving the interactions between objects to be carried and the human, the DBM offers a unique tool for evaluating both the specific effect of a particular piece of kit and cumulative effects of carrying multiple loads.

In the current study, a 3D solid model was split into an upper and lower torso coupled with a rigid joint. This joint was located at the approximate location of the spine and the L3/L2 height. Previous models had been constrained to move along a single axis and had used a simple sinusoid function. The model was modified to use a table of values from experimental data to control the motion of the torso. Acceleration histories of subjects wearing packs were previously recorded during human trials (Morin et al, 2002). These consisted of simultaneous recordings of the acceleration of the subject’s sternum and the simultaneous acceleration history of the pack. The acceleration histories of the person have been numerically integrated and used to drive the motion of the DBM torso. Since accelerations for a wide range of activities were recorded and can be used to drive these models, an excellent data base for many human and pack motions exist for current and future modeling of human motions. This technique of capturing and generating motions is applicable to many situations where an envelope of human motions and body accelerations need to be tested to ensure equipment does not cause excessive dynamic loading on the human. The DBM is not only a model of a load carriage system. It is also a model of a human form that determines the effect of different equipment on a set of biomechanical factors when the torso moves through a range of soldier motions.

A series of piecewise linear dynamic, static and creep material response models was developed for materials present in typical shoulder straps, hip belts, and padding. In addition to these models for individual components, a piecewise linear model of the stress-strain response for the CTS shoulder strap assembly was developed for inclusion in the DBM.

Provisions were made for the model to estimate reaction forces and moments on the lumbar spine and the total shoulder reaction force. The model also calculates the distribution of force to the upper and lower torso and the total contact force.

Work is proceeding on incorporating a skin layer and creating the ability to examine interaction details at the equipment - skin interface. The final goal is to estimate injury risk potential across a range of activities and loads.

## Sommaire

L'objectif global du programme de recherche sur la modélisation biomécanique dynamique menée par RDDC consiste à améliorer la compréhension des capacités humaines de transport de charge et à comprendre les effets des caractéristiques nominales de systèmes de transport de charge sur la santé et la mobilité humaines. De plus, la présente étude vise à élaborer une méthode pour déterminer plusieurs facteurs biomécaniques qui pourraient être utilisés comme paramètres d'entrée dans le modèle de limite de charge décrit dans le rapport de RDDC n° W7711—0-7632-01 intitulé « Plan à long terme proposé pour le programme de recherche et de développement d'un modèle dynamique de transport de charge ».

Les phases antérieures de la modélisation biomécanique dynamique ont permis de comprendre les modèles dans lesquels l'interface objet-personne est examinée sous l'angle de la pression de contact. Grâce à sa résolution des interactions entre les objets à transporter et l'humain, le DBM est un outil unique pour l'évaluation de l'effet précis du transport d'un élément particulier du fourbi et des effets cumulatifs du transport de charges multiples.

Dans l'étude, un modèle volumique de torse a été scindé en un torse supérieur et en un torse inférieur reliés par un joint rigide, qui a été placé approximativement à la hauteur des vertèbres L3/L2 de la colonne vertébrale. Dans les modèles antérieurs, le mouvement était restreint à un seul axe, et une fonction sinusoïdale simple était utilisée. Le modèle a été modifié de manière à utiliser une table de valeurs expérimentales pour commander le mouvement du torse. Durant des essais effectués sur des humains, on a consigné l'historique des accélérations de sujets équipés de sac à dos (Morin et al, 2002). L'historique était composé des enregistrements simultanés de l'accélération du sternum du sujet et de l'historique d'accélération simultanée du sac à dos. Les accélérations de la personne ont été intégrées numériquement et ont été utilisées pour réaliser le mouvement du torse pour le DBM. Les valeurs d'accélération du torse ont été consignées pour un grand nombre d'activités et elles peuvent servir à alimenter les modèles pour ces activités et ainsi créer une excellente base de données contenant bon nombre de mouvements humains et de sacs en vue de la modélisation en cours et future des mouvements humains. Cette technique de saisie et de production de mouvements s'applique à un grand nombre de situations où il faut tester une enveloppe de mouvements humains et d'accélérations corporelles afin de s'assurer que l'équipement ne constitue pas une charge dynamique excessive pour l'humain. Le DBM est à la fois un modèle de transport de charge et un modèle de corps humain qui permet de déterminer l'effet de différents types d'équipement sur un ensemble de facteurs biomécaniques grâce au déplacement du torse dans la gamme de mouvements effectués par les soldats.

On a élaboré des modèles linéaires par morceaux de la réponse dynamique, de la réponse statique et du fluage pour les matériaux types utilisés dans la fabrication des sangles d'épaule, des sangles de hanches et du matelassage des sacs à dos. En plus des modèles des éléments individuels, un modèle linéaire par morceaux de réponse à l'effort-déformation de l'ensemble de sangles d'épaule du HLS a été développé pour fins d'inclusion dans le DBM.

Le modèle permet d'évaluer les forces de réaction et les moments sur la colonne lombaire et la force de réaction globale des épaules. Il permet également de calculer la répartition de la force entre le torse supérieur et le torse inférieur et la force totale de contact.

Les travaux sont en cours en vue de l'intégration d'une couche de peau, ce qui permettrait d'examiner en détail l'interaction au niveau de l'interface équipement-peau. Le but consiste à évaluer les risques de blessures pour une gamme d'activités et de charges.





# Table of Contents

Abstract .....	i
Résumé.....	ii
Executive Summary .....	iii
Sommaire .....	iv
Table of Contents.....	vii
List of Figures .....	ix
List of Tables .....	x
1.0 Background.....	1
2.0 Phase IV DBM 3D Model Description.....	3
2.1 Direction of current work.....	4
3.0 Application of modeling .....	5
3.1 Identification of potential human injury risk modes.....	5
4.0 Description of Current Model.....	6
4.1 Split torso .....	6
4.2 Physical properties of the model.....	7
4.2.1 Moment of inertia .....	7
4.2.2 Centre of mass.....	8
4.2.3 Friction.....	8
4.2.4 Coefficient of restitution .....	8
4.2.5 Shoulder straps.....	8
4.2.6 Composite foam studies.....	8
4.2.7 Creep Studies .....	11
4.2.8 Dynamic Response of Shoulder Strap Assembly .....	13
4.3 Development of Forcing Function .....	15
4.3.1 Inputting the Forcing Function .....	19
5.0 Model Outputs .....	20
5.1 Critical factor outputs .....	20
5.2 Contact forces on body .....	22
5.3 Distribution of forces between upper and lower torso.....	23
5.3.1 L5/S1 shear force .....	23

6.0 Continuing Development .....	24
6.1 Modeling interface contact pressures on human skin .....	24
7.0 References .....	25
Appendix A - Compression Testing of Five Foam Materials .....	A-1
Scope .....	A-2
A1) Test Description .....	A-2
A1.1) Test Equipment .....	A-2
A1.2) Test Samples .....	A-3
A1.3) Test Loading Patterns .....	A-3
A1.3.1) Dynamic testing .....	A-3
A1.3.2) Creep Testing .....	A-3
A1.4) Test Methods .....	A-5
A2) Test Results .....	A-5
A2.1) Dynamic Testing .....	A-5
A2.1.1) Cyclic Frequency of 1.8 Hz .....	A-5
A2.2) Dynamic Testing .....	A-6
A2.2.1) Cyclic Frequency of 3.5 Hz .....	A-6
A2.3) Creep Testing .....	A-7
Appendix B - Calculation of Torso lean from acceleration .....	B-1
Appendix C - Details of the Suspension Testing Jig .....	C-1

## List of Figures

Figure 1	Upper and Lower Torso Segments .....	7
Figure 2	Elastic Moduli under cyclic loading, 1.8 Hz.....	10
Figure 3	Detail of Creep response – CTS Shoulder Pad .....	11
Figure 4	Shoulder Pad Linearized Creep Response .....	12
Figure 5	Test Setup for Dynamic Test of CTS Suspension system .....	13
Figure 6	Applied Load and Extension of Shoulder Suspension System.....	14
Figure 7	Force Extension Curve - Shoulder Suspension System.....	14
Figure 8	Detail of the Suspension System Cyclic Loading Response .....	15
Figure 9	Medial Lateral Accelerations during Boulder Hop.....	17
Figure 10	Medial Lateral Velocity during Boulder Hop.....	17
Figure 11	Error Compensated, Medial Lateral Velocity during Boulder Hop.....	18
Figure 12	Creation of Prescribed Velocity Profiles .....	19
Figure 13	Side view of walking model .....	20
Figure 14	Plane view of walking model.....	21
Figure 15	Contact force on torso during walking.....	22
Figure 16	Estimated Forces at L5/S1 .....	23
Figure A-1	Material Testing System.....	A-2
Figure A-2	Foam specimens .....	A-3
Figure A-3	Test Profile for Dynamic tests.....	A-4
Figure A-4	Test Profile for Creep tests.....	A-4
Figure B-1	Accelerometer Orientation in the Earths’ Gravitational Field .....	B-1
Figure C-1	Detail of Upper Attachment.....	C-1
Figure C-2	Detail of Lower Attachment .....	C-2
Figure C-3	Suspension Tester .....	C-3

## List of Tables

Table 1	Moments of Inertia and Geometry- CTS Pack .....	8
Table 2	Location of Centre of Mass- CTS Pack .....	8
Table 3	Sample Thickness and Range of Deflection .....	9
Table 4	Young's Modulus for Foams .....	10
Table 5	Summary of Creep Strain Characterization for CTS Shoulder Pad.....	12
Table 6	Summary of Force Extension Characterization of CTS Shoulder Suspension System.....	15
Table A-1:	Target versus actual results .....	A-5
Table A-2:	Deflection Range for cycling at 1.8 Hz .....	A-5
Table A-3:	Young's Modulus for each sample.....	A-6
Table A-4:	Target versus actual results.....	A-6
Table A-5:	Deflection Range for cycling at 3.5 Hz .....	A-6
Table A-6:	Young's Modulus for each sample.....	A-7
Table A-7:	Slope of displacement versus time c .....	A-7

## 1.0 Background

The Dynamic Biomechanical Model (DBM) is being developed in support of the creation of a Load Carriage Limit model. This is an equation that would take into account key factors that effect the load a soldier could carry based on task conditions (especially time or distance). Factors suggested in the model were: physiological factors, biomechanical factors, demographic factors and readiness factors. For a more complete description of the Load Conditions Limit model and underlying assumptions, please see the DRDC report # W7711—0-7632-01 entitled “Proposed Long Range Plan for a Research and Development Program of Dynamic Load Carriage Modeling”. As part of the supporting work for the development of the biomechanical factor, a dynamic biomechanical model of a soldier and their equipment is being developed to generate a number of estimates for biomechanical pack and human load carriage variables.

The purpose of this work is to develop a dynamic biomechanical model capable of providing accurate pack-person interface information when provided with geometry and material property inputs.

Previous phases of dynamic biomechanical modeling research have led to an understanding of modeling that treats object-person interfaces as an interface contact pressure problem. In solving the interactions between objects to be carried and the human, the DBM offers a unique tool for evaluating both the specific effect of a particular piece of kit and cumulative effects of carrying multiple loads.

Human load carriage of any item has the following aspects:

- Control of the objects’ motion
- Increased forces on musculature for control and carriage
- Interface pressures between the body and the object

Each of these parameters must be managed well to minimize the effect on the body. Although the initial thrust for the Dynamic Biomechanical Model arose from the exploration of pack based load carriage systems, lessons learned are applicable across a range of interfaces and load scenarios. The effect of any object carried on any part of the body may be thought of in terms of interface pressures applied to the body surface and transmission paths of these forces through the skeletal system. Successful understanding and modeling of this interface may permit the prediction of interface pressures from the motion of the system.

### ***Dynamic Biomechanical Model***

Previous research has shown that biomechanical factors such as shoulder and lumbar reaction force as well as skin contact pressures are strongly correlated to physical discomfort when wearing a backpack (Stevenson et al., 1996, 1998). The Ergonomics Research Group had developed static backpack models (Stevenson et al., 1996; Pelot et al., 1999) that provide these output measures. These models could not be extended to include complex waist belts because this model became statically indeterminate, (i.e. had more unknowns than independent equations based on the external geometry). As well as the more complex geometry, the material properties and the effect of varying them could not be gauged with a simple static model. The decision was made to purchase integrated

dynamic motion and stress analysis software to increase the types of analysis possible and to allow greater input flexibility for users.

As systems become more complex, they often become statically indeterminate meaning that there are insufficient relationships defined by the static geometry to uniquely define all the system variables. One approach to this problem is to assume linearly elastic material behaviours and apply the resulting displacement relationships to provide additional equations. These deformation constraints result from the fact that in structural systems, connected elements must deform such that they satisfy the final system geometry. Using the material properties and displacement constraints, additional relationships can be derived to help arrive at a determinate system. As well, in a dynamic situation, system accelerations are not equal to zero and the motion of components must be included in the formulation of system equilibrium equations. Sophisticated software programs automate the generation of these constitutive equations and are a distinct advantage when multiple geometries and material properties are examined.

When the resultant material properties of composite materials are not easily measured, an additional solution method has developed. Characteristics of a suspension system can be determined by knowing both the resultant motion of a body and the input function. In this way, the characteristics of a LC suspension system can be inferred by knowing the forcing function and the resultant pack motion. This gross behaviour is then modeled by combining mathematical expressions to replicate the motion recorded. These mathematical expressions relate to the physical world in that parameters, such as coefficients of damping or friction, are measurable properties of the load carriage suspension interface. In order to reduce the number of possible solutions, specific elements of the pack, (i.e., shoulder straps) were tested under isolated conditions to determine their stress-strain response characteristics under load. A complete description of this testing appears in Appendix 1. The force displacement and creep response of these and other elements allow us to describe the mechanical characteristics of pack components as combinations of linear and/or non-linear springs and linear and/or non-linear dampers. Then, knowing the input function (person's motion) and output (pack) motions, we can model the interface by using a series of appropriate elements in equations that represent the response function.

## 2.0 Phase IV DBM 3D Model Description

Model inputs:

1. Velocity histories of a person wearing a pack
2. Stiffness of the shoulder straps
3. Stiffness of the lumbar pad and back panel

Model Outputs:

1. Estimated shoulder reaction forces
2. Estimated lumbar forces
3. Ratio of load carried in upper body / lower torso
4. Contact force on upper torso
5. Contact force on lower torso
6. Pack and person motion in 3D

Previously, the DBM model used a solid 3 dimensional torso shape based on a surface scan of the 50 percentile male mannequin. Contact with the torso was lumped together and reported in terms of forces acting on the centre of mass of the body. The Phase IV model required more refinement of the torso to allow the analysis to report contact forces specific to the upper and lower torso.

Determining the stress state of the spine in the lumbar area required the creation of separate upper and lower torso segments. The 50 percentile male body shape was split graphically into two solid objects at the approximate vertical location of L5/S1 using Mechanical® Desktop. These objects were first saved as STP files and then imported into the dynamic modeller, VisualNastran 4D® (VN4D). A rigid joint, which transmits all forces and moments, was created between the upper and lower body segments at the approximate location of the spine. The model now outputs upper and lower body contact forces separately. As well, this modification permits the model to determine lumbar shear forces.

At the base of the model is a second constraint that restricts the motion of the torso. Care must be taken to ensure that the model is neither over nor under constrained. If a model is over constrained, the solution will be forced to take a particular form. If under constrained, an infinite number of solutions will exist for a given set of input conditions. In motion 1, walking, the torso was defined to be free to move in the X, Y and Z directions. It was also free to rotate about its' fore/aft axis (Y axis). Prescribing displacement in the X, Y and Z directions, provides constraint to these axis of motion. Depending on the motion being modelled, different degrees of freedom may be constrained to allow the correct motion to occur and properly constrain the model in space.

For this work, a rectangular representative pack was created based on the geometry of the CTS pack and consistent with the pack models used in the previous 2 and 3D analyses. The moments of inertia about the X, Y and Z axes were defined based on the moments of inertia of the CTS pack used for the human trials and measured using a moment of inertia platform (trifilar pendulum).

Shoulder straps were modeled as a Voigt-Kelvin visco-elastic material with a stiff linear spring in series with a linear damper to reproduce the combined effect of a compliant shoulder pad and stiff webbing material.

## **2.1 Direction of current work**

The current work has focussed on integrating motion profiles recorded during the human trials circuit, December 2001 (Stevenson et al, 2002). In these trials, subjects wore battle and marching orders under different load conditions. One accelerometer was mounted on the sternum of the person and a second was attached to the backpack frame sheet. In addition, strain gauges were used to record strap tensions in the shoulder straps and waist belt. This report will describe how this information has been used to form a partial data set (accelerations, velocities, displacements and strap forces) for development and validation of the DBM.



### 3.0 Application of modeling

This particular model and the underlying capabilities are being developed to support the general goal of furthering the understanding of person-to-equipment interactions and with the specific goals of integrating current understanding of human biomechanical limits with the particular demands of backpack load carriage. The goal is to use this type of analysis to evaluate the effect of different loads and load carriage devices on the ability of the soldier to perform. The combined effects of contact pressures, shoulder and lumbar forces and load distribution onto the body, examined across a wide range of required motions will be distilled into a biomechanical load multiplication factor. This factor will be used to estimate the net effect of equipment on a soldiers' expected performance. The techniques used are not confined to backpacks but are applicable to other devices mounted or carried on the human body.

#### 3.1 Identification of potential human injury risk modes

Identification of potential injury modes forms the benchmark against which biomechanical stresses can be evaluated. Once quantified, these injury risk modes will be used to evaluate cumulative effects of load carriage and specific effects of different devices. Risk modes fall into the following general categories:

- Back and spinal injury
- Lower limb injury (maximum moment and force values)
- Connective tissue injury, ligaments and tendons
- Wear injury, cumulative effects of load, activity and fatigue
- Skin and subcutaneous injury due to constant pressure

The US Army is also pursuing a similar model for the application of biomechanical modeling; the following paragraph is taken from the current U.S. Army Aeromedical Research Laboratory website:

***Injury Science and Systems Hazards Research<sup>1</sup>***

*Principal Laboratory: U.S. Army Aeromedical Research Laboratory*

*During training and deployment, soldiers are at risk for injury, incapacitation, and degraded performance resulting from inhaled toxic gases, blunt trauma, whole body blast effects, directed energy, stress fracture, vehicle jolt, and load carriage effects. The study of each of these effects is leading to the development of an integrated biomechanical model of injury and fatigue. Presently, articulated models of the head and neck are being developed to define the manner and amount of head-supported mass that soldiers can sustain without risk of injury or performance deficits due to muscle fatigue. These models are critical, particularly for Army aviators, for the exploitation of helmet-mounted display technology and head and eye protection devices....*

---

<sup>1</sup> <http://mrmc-www.army.mil/index.asp?EntryURL=/mrdRADs.asp>

A significant body of research exists on injury modes such as lower back and spinal injury, cumulative effects of lifting and repetitive activity while areas such as skin pressure and subcutaneous tissue injury have not been studied extensively in healthy, fit subjects subjected to the magnitude or durations typical in military load carriage. (McGill, 2002) The DBM is being developed to relate the effects of any load to these injury modes. Information from literature (Edsberg et al 1999, Mak, et al 1994), and ongoing research in pressure tolerance (Stevenson, Morin et al, Proposal for TIES Funding, 2003-2004, Development of The Dynamic Biomechanical Model by Means of the Portable Measurement System, submitted May 21, 2003) will provide additional pressure injury guidelines for this and other biomechanical models.

## **4.0 Description of Current Model**

### **4.1. Split torso**

Previously (Reid, 2002), the DBM used the 3D geometry of the Load Carriage simulator mannequin. This torso model consisted of a single rigid body. VisualNastran 4D (VN4D) requires that the geometry of all regions be defined separately. The torso will be subdivided as needed to add either material property detail or to separate constraint conditions. In this contract, the torso shape has been separated into an upper and a lower portion at approximately the L5/S1 level. This permits separate calculation of the forces and moments for the upper and lower torso. The geometry of the torso shape was modified using Unigraphics® and exported into the VN4D platform. This is required because VN4D has only rudimentary shape creation abilities, relying on other computer aided design software to provide detailed geometries.

The location of the centre of rotation of the spine was estimated and a rigid joint was created at this position. This rigid joint transmits all forces and moments and does not allow relative movement between the connected upper and lower torsos. Figure 1 shows the location of this rigid link and the separation of the upper and lower torso segments. Petit (2002) created a fully articulating multi-body spine model which modeled vertebral bodies as connected by revolute joints constrained by three orthogonal springs with its' rotation about the average centre of rotation for all movements at that joint. This level of detail could readily be incorporated into the current joint model if further refinement proves desirable.

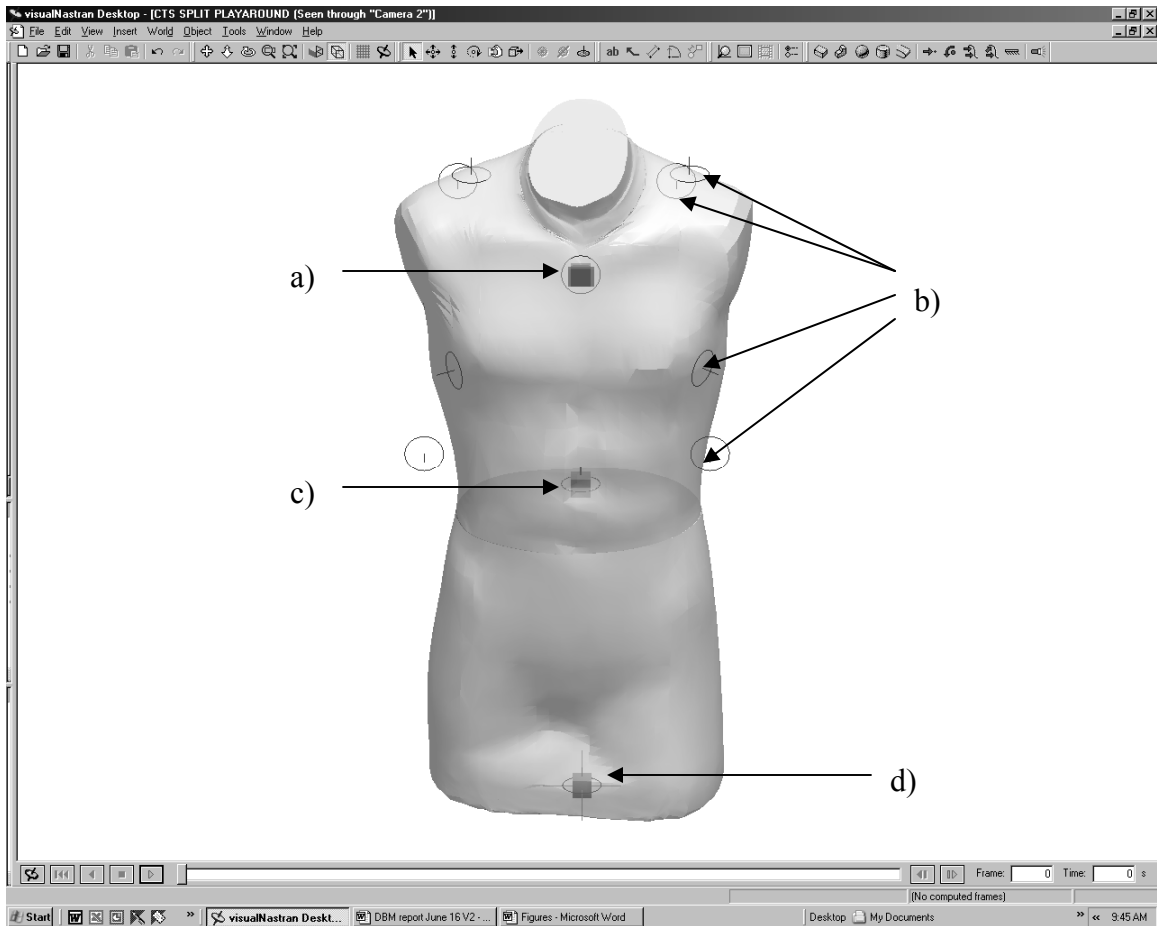


Figure 1 Upper and Lower Torso Segments

- a) Accelerometer location
- b) Attachment points of shoulder straps
- c) Rigid joint between upper and lower torso
- d) Support constraint location

## 4.2 Physical properties of the model

### 4.2.1 Moment of inertia

Although the upper and lower torso objects have the outward appearance of a human body, internally they are assumed to be homogenous solids. As the displacement of the torso is controlled by the input displacement files, no additional refinement of the torso inertial parameters is required at this time. The CTS pack model does require a complete definition of its' moment of inertia to resolve the packs' response to the torso's motion.

Pack model dimensions and inertial properties were based on the CTS nominal 25 kg load used in the human trial (Stevenson et al, 2002). A summary of the pack models' geometry and inertial properties is given in Table 1.

Table 1 Moments of Inertia and Geometry- CTS Pack

	$I_{xx}$	$I_{yy}$	$I_{zz}$
CTS Pack model	0.240 kg.m <sup>2</sup>	0.223 kg.m <sup>2</sup>	0.125 kg.m <sup>2</sup>
CTS Pack in Trial	0.240 kg.m <sup>2</sup>	0.223 kg.m <sup>2</sup>	0.125 kg.m <sup>2</sup>
Geometry	X (Width)	Y (Depth)	Z (Height)
CTS Pack model	0.35 m	0.26 m	0.63 m

#### 4.2.2 Centre of mass

The centre of mass of the CTS pack was automatically located at the centre of the pack volume based on the defined moments of inertia and an assumption of uniform density. The pack worn by the soldiers in the human trial had a centre of mass located as described in Table 2.

Table 2 Location of Centre of Mass- CTS Pack

	Height from base	Distance from frame	Medial/lateral offset
CTS Pack model	0.315 m	0.130 m	0.00 m
CTS Pack in Trial	0.267 m	0.123 m	0.02 m

#### 4.2.3 Friction

Sanders et al. (1998) measured the coefficient of friction (COF) of skin with socks to be 0.75 +/-0.09 while Naylor (1955) reported a range of values depending on the level of moisture on the skin; dry skin has a COF of 0.6 and sweat increased the COF to 1.00. The pack and torso were defined with a COF of 0.9, which is consistent with damp skin.

#### 4.2.4 Coefficient of restitution

The coefficient of restitution describes the result of a collision between two bodies. It is defined as the ratio of the resulting velocity compared to an objects original velocity. If the collision is completely elastic, the bodies would have a coefficient of restitution of 1 and would rebound with the same velocity they had prior to the collision. Bodies with a coefficient of restitution of 0.0 would stay in contact. The torso and the pack are defined as having a coefficient of restitution of 0.5.

#### 4.2.5 Shoulder straps

Strap constraints as currently modeled depend on the relative position of the strap end points to determine if the strap is relaxed (applying no load) or in tension. The distance between the two ends of the constraint is compared to the natural rest length of the constraint and no force is applied unless this length indicates that the strap would be in tension.

#### 4.2.6 Composite foam studies

The waist belt, lumbar pad, portions of the frame sheet and the shoulder straps are constructed out of one or more layers of manmade foam rubber. These structures create the ability to control load motion by having sufficient stiffness in the required orientations but still must provide suitable load transfer to the body. To achieve this, intricate combinations of materials and geometries are combined create a structure that achieves the overall desired behaviour. Structures can be modeled by creating an exact geometric

model of each subcomponent and assigning individual material properties (compressive strength, stiffness, etc.) to each part. Depending on the complexity of construction, the resulting model may become unwieldy or inaccurate due to accumulated errors. An alternative is to model the lumbar pad or waist belt object as having a “composite” set of material properties. To do this, a custom material is created for the model that has for its material properties, the resultant behaviour of the assembled part.

Two series of tests were conducted to create a library of materials available for modeling. The first series was the testing of four foam specimens and a CTS shoulder pad for compression, creep and dynamic performance. The second series of tests examined the creep behaviour of these materials. These data will be used when it is necessary to model individual foam components. A small number of foams were selected as common backpack construction materials. They are used in waistbelts, lumbar pads, on framesheets and in shoulder pads. A complete description of the foam testing appears in Appendix 1 of this report. Four different materials and one composite material were tested. These were; Trocellan, Volara, EVA (Ethylene Vinyl Acetate), Ether foam and the CTS shoulder strap. A description of the materials tested and the typical compression displacement appears in Table 3.

Table 3 Sample Thickness and Range of Deflection

<b>Sample</b>	<b>Min-Max Deflection (mm)</b>	<b>Sample Thickness (mm)</b>	<b>Percent Deflection</b>
Trocellan (polyolefin)	1.0-1.2	6.3	16 - 19%
Volara (ethylene/ether)	1.3-2.9	5.8	22 – 50%
EVA Ethylene Vinyl Acetate	3.1-5.3	14.1	22 – 38%
Urethane/Ether	8.5-9.0	10.9	78 – 83%
Strap	11.0-16.0	26.1	42 – 61%

Two calculations for the elastic modulus (E) were performed and a summary of the testing appears in Table 4. First, the slope of the stress strain-curves at the point of the initial unloading was calculated for one cycle of each sample and appears as column 2 of Table 4. This calculation is based on a typical procedure for calculating E in tension. Upon cyclic loading, all materials tested demonstrated a degree of hysteresis and creep. For the purposes of the DBM, variation in stiffness between compression and decompression will have a small effect and initially an averaged response is sufficient to estimate stress in the material. These facts lead to a second analysis. To determine the average response, a linear regression was performed for multiple test cycles ( $n \geq 50$ ). When this test was repeated at a higher frequency, results showed all materials were strain rate dependant with E increasing at higher load/unload cycle frequency. These results appear in columns 3 and 4 of Table 4. Compression behaviour at 1.8 Hz is shown in Figure 7. Figure 8a shows the response of the same materials at approximately 3.2 Hz. Additional details of this testing and analysis appear in Appendix A.

Table 4 Young's Modulus for Foams

Sample	Initial E Unloading (kPa)	Avg. E (kPa) 1.8 Hz Load/Unload	Avg. E (kPa) 3.2 Hz Load/Unload,
EVA	378.6	290.6	388.1
Volara	398.5	289.9	318.3
Strap	2720.3	722.5	905.7
Trocellan	3287.3	1957.9	2036.9
Ether	4204.5	1602.0	1747.5

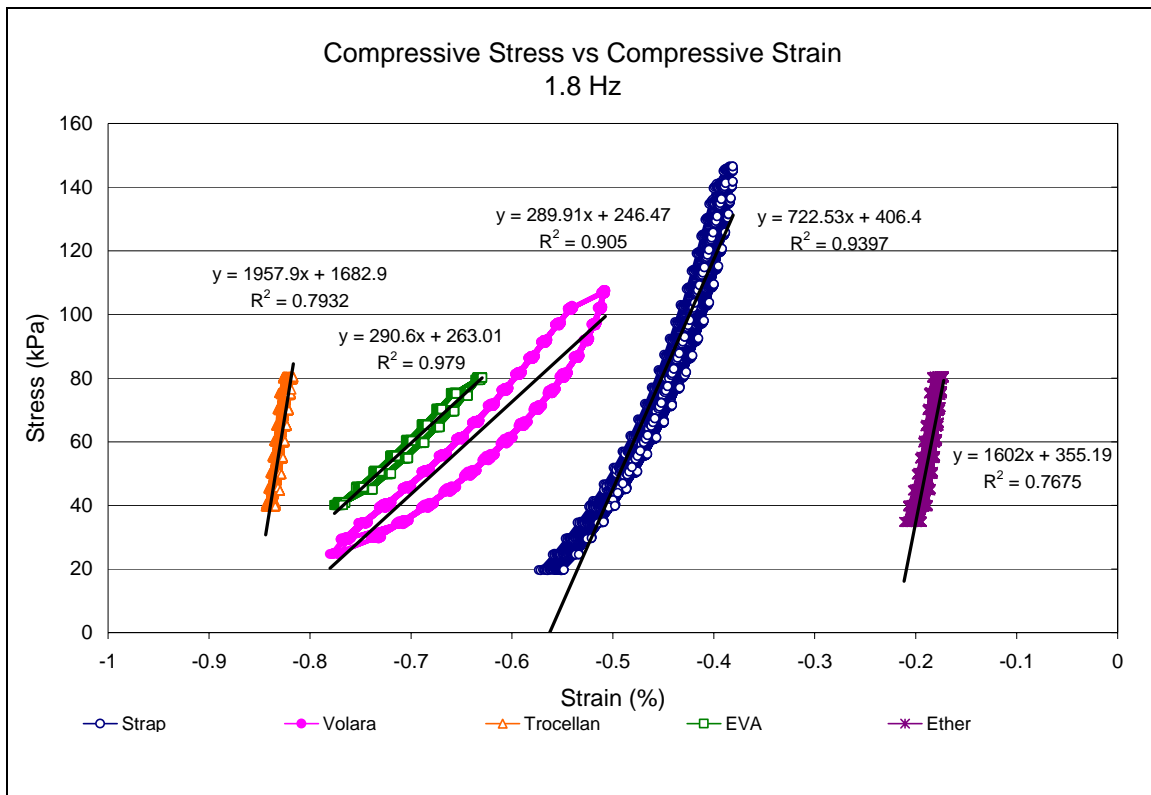


Figure 2 Elastic Moduli under cyclic loading, 1.8 Hz

Determination of an average elastic modulus based on multiple loads at 1.8 Hz. All samples show some degree of hysteresis and creep.

#### 4.2.7 Creep Studies

##### Creep Response

Materials subjected to continuous loading may show an increased displacement (compression) over time with no increase in load. This behaviour, known as creep, may lead to a loss in the ability to distribute loads to the underlying tissue as the foam compresses to the point where portions act as a solid. When subjected to a range of typical backpacking loads, all the foams tested demonstrated some creep. Figure 3 shows a portion of the creep response of the shoulder strap under 60 kPa load. In approximately 100 seconds, the pad thickness decreases by approximately 0.8 mm, 3% of its' 26mm original thickness.

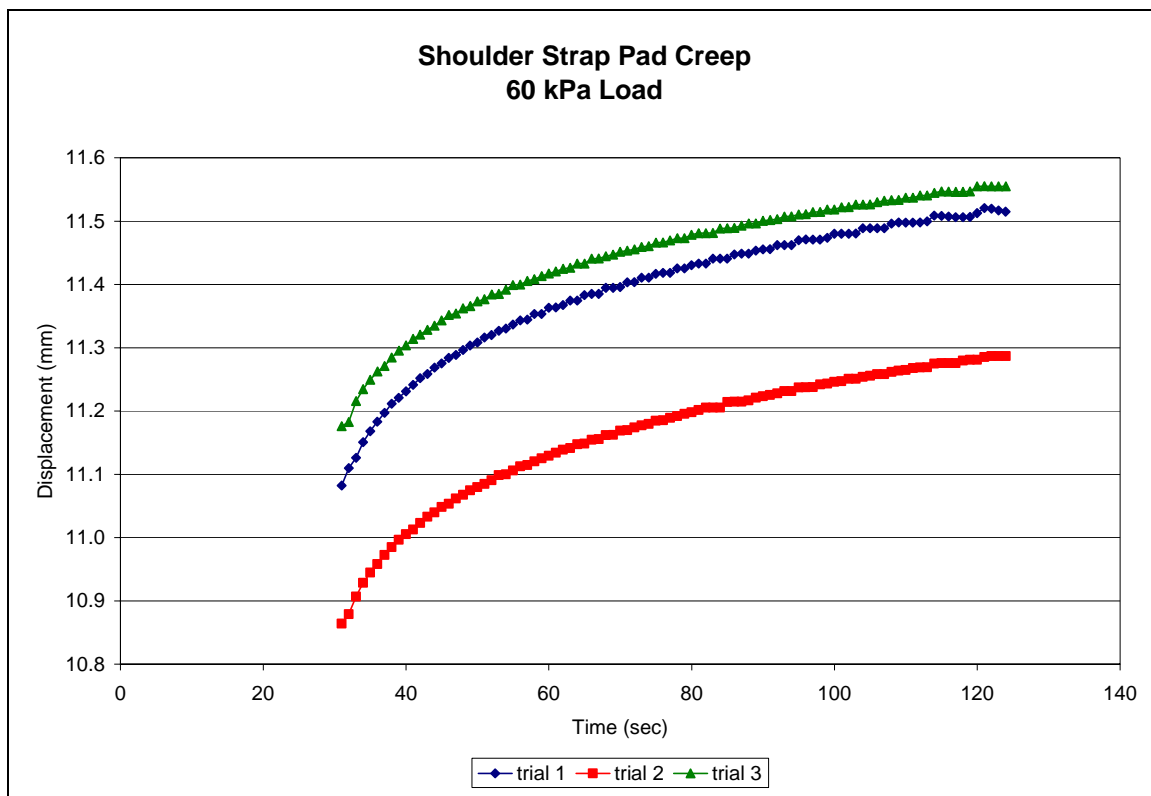


Figure 3 Detail of Creep response – CTS Shoulder Pad

A creep model was created from testing the shoulder strap foams at 20, 40 and 60 kPa compression load. A typical response of the shoulder pad is shown in Figure 4 where percent strain is plotted against time for a constant 60 kPa pressure. Results for the creep testing of individual foams (Trocellan, Volara, EVA and Ether) are included in Appendix 1 of this document.

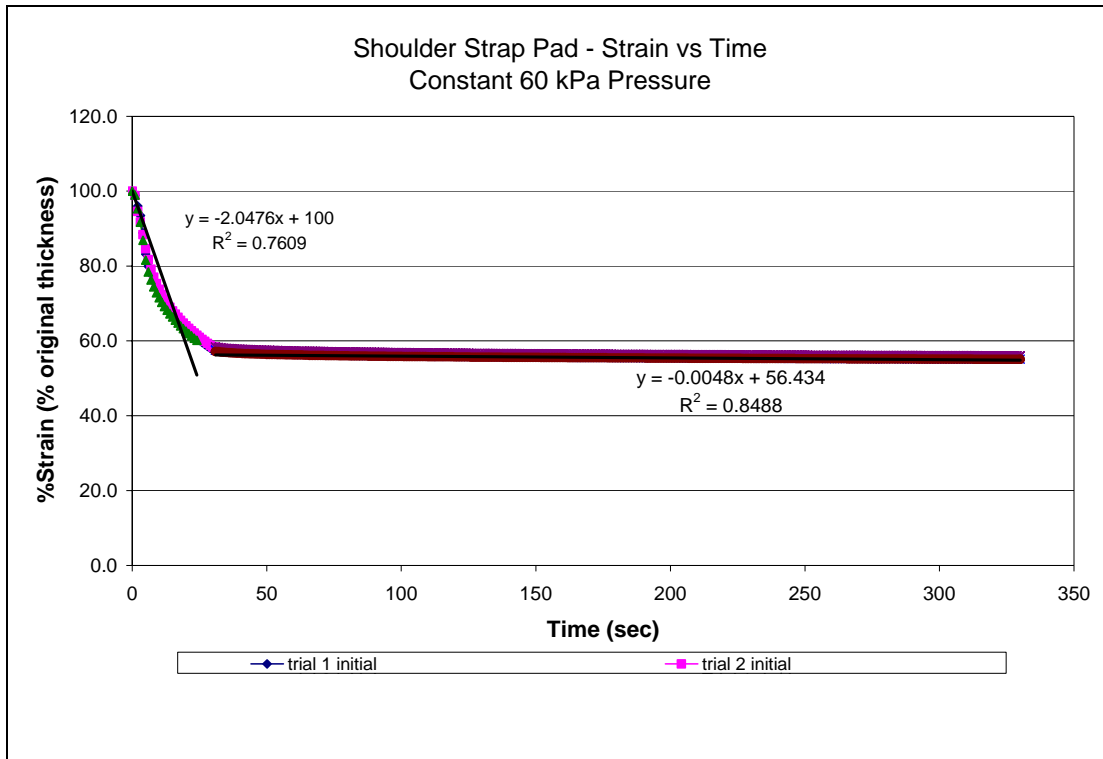


Figure 4 Shoulder Pad Linearized Creep Response

This response was modeled as 2 phase, piecewise linear. Initially strain,  $e_o$ , changes rapidly with time until a transition phase. At this point, the strain rate  $\dot{\epsilon}_{ss}$  approaches steady state. The material is strain rate sensitive as shown by the variation in the values calculated for the creep response under different pressures. Linear interpolation will be used to calculate intermediate values between the test pressure loads to determine a strain state for intermediate pressures. A summary of the creep time constants for the shoulder strap pad appears in Table 5.

Table 5 Summary of Creep Strain Characterization for CTS Shoulder Pad

Applied Pressure	Initial Strain $e_o$	Creep Strain $\dot{\epsilon}_{ss}$	Time of Transition $t$ (sec)	Strap model Equation
20 kPa	$-1.1395t + 100$	$-0.0059t$	26.322	For $0 \leq t \leq 26.32$ $e_o = -1.1395t + 100$ For $t > 26.32$ $\epsilon(t) = -0.0059t + 29.6400$
40 kPa	$-1.4936t + 100$	$-0.0047t$	26.402	For $0 \leq t \leq 26.40$ $e_o = -1.4936t + 100$ For $t > 26.40$ $\epsilon(t) = -0.0047t + 39.283$
60 kPa	$-2.0476t + 100$	$-0.0048t$	21.367	For $0 \leq t \leq 21.367$ $e_o = -2.0476t + 100$ For $t > 21.367$ $\epsilon(t) = -0.0048t + 43.668$



#### 4.2.8 Dynamic Response of Shoulder Strap Assembly

Although it is possible to create a model of a shoulder strap assembly by joining or layering together individual components, this may not be the most effective way to proceed. It may be preferable to test a complete assembly of the shoulder suspension system and model the overall system response empirically. An apparatus was designed to test the resulting dynamic response of the shoulder strap with padding and webbing combined. Compliance of upper and lower attachment points on the bag and the webbing would have to be tested separately and modelled individually to exactly replicate the physical system.

It is possible to perform a global test and model each system of shoulder straps using the pooled dynamic behaviour. A second series of tests looked at the dynamic performance of the composite shoulder straps, including the webbing, padding, load lifters straps and yoke on the CTS pack. A device (see Figure 5) was built to hold the shoulder straps and yoke at an angle that allowed the Instron® Universal Testing machine to apply the tensile load in the same orientation as gravity. The upper attachment was designed to mimic the way that load would be applied to the shoulder straps. It was fashioned out of 152.5 mm diameter hollow tubing covered with a 2mm layer of Bocklite® to provide a uniform nonzero coefficient of friction. Connection to the Instron Load cell was with a universal joint to provide pure tension. Additional details on the test jig construction are contained in Appendix 3.



Figure 5 Test Setup for Dynamic Test of CTS Suspension system

The loading pattern was  $225\text{N} \pm 25\text{N}$  (100 to 125 N per each shoulder) and was based on a typical strap loads measured during load carriage simulator testing for a 25 kg backpack load. Load was ramped slowly up to 90% maximum, held for 5 seconds, and

then oscillated at 1.8 Hz. Results of dynamic testing of the suspension system appear in Figures 6. Figures 7 and 8 show the results and the development of a linearized stress strain model for this data.

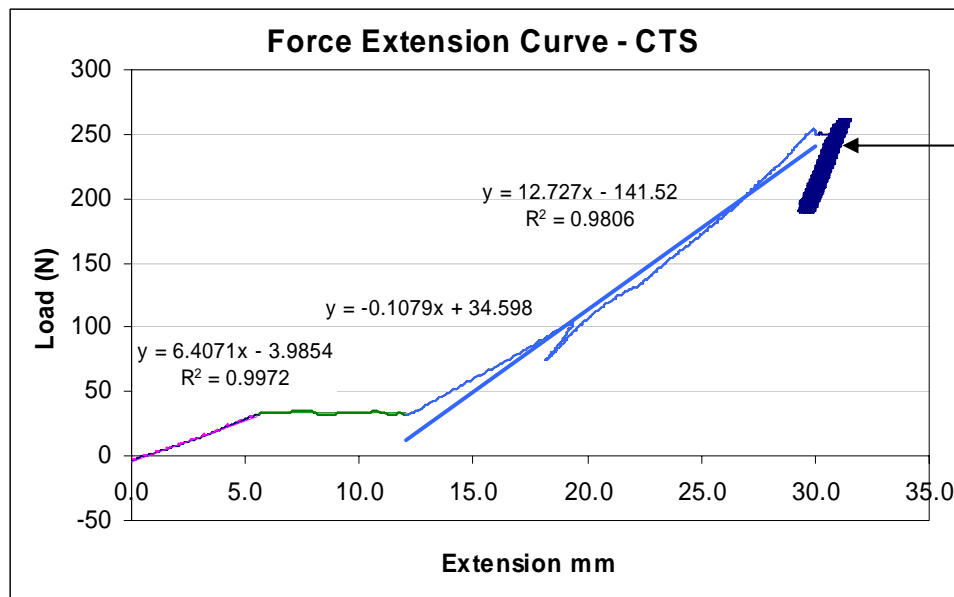


Figure 6 Applied Load and Extension of Shoulder Suspension System

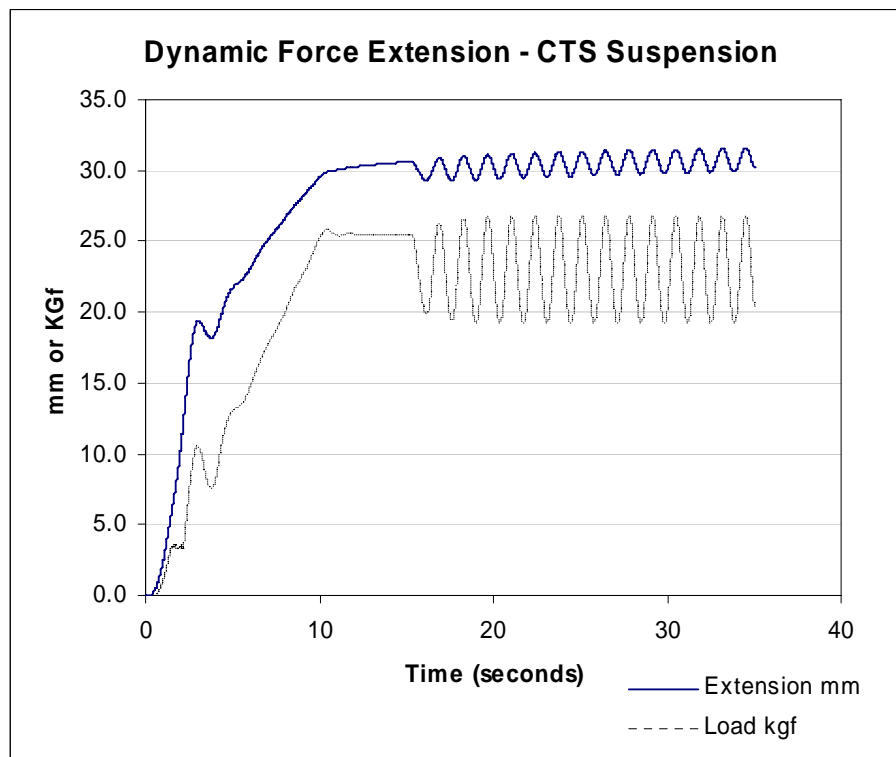


Figure 7 Force Extension Curve - Shoulder Suspension System  
System response approximated by a piecewise linear stress strain model.

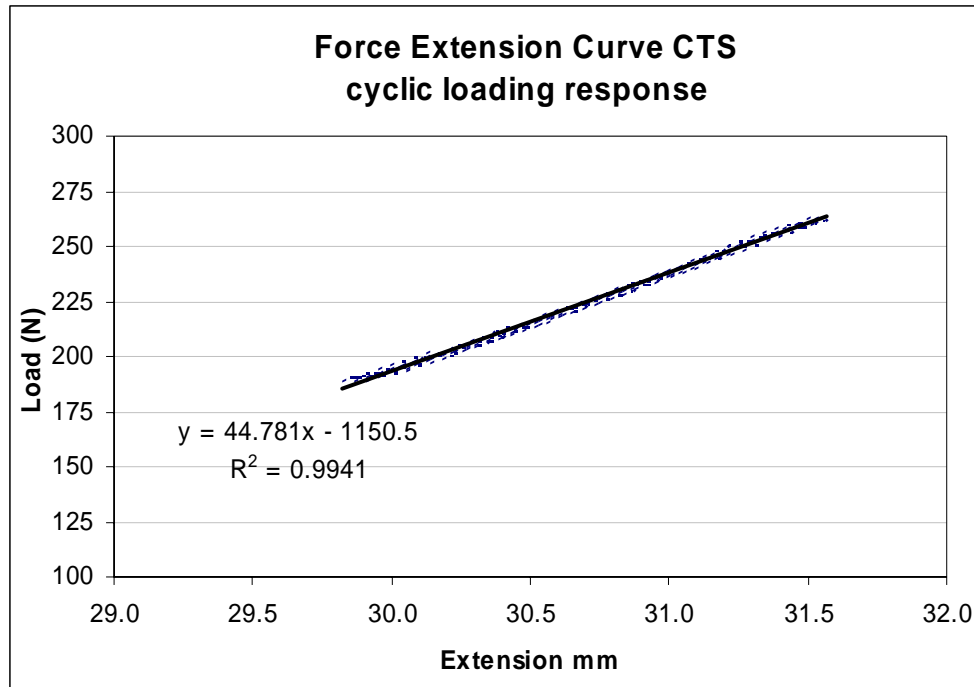


Figure 8 Detail of the Suspension System Cyclic Loading Response

As is apparent in Figure 7, the force extension behaviour of the shoulder strap appears as a series of linear regions. This data formed the basis for developing a piecewise linear force/extension model. A summary of the suspension system model appears in Table 6.

Table 6 Summary of Force Extension Characterization of CTS Shoulder Suspension System

Extension (e) mm	Force (N)
$0 \leq e \leq 5$	$F = 6.407e - 3.99$
$5 < e \leq 12$	$F = -0.108e + 34.59$
$12 < e \leq 30$	$F = 12.727e - 141.52$
$29 < e$	$F = 44.781e - 1150.50$

### 4.3 Development of Forcing Function

Accelerations from human testing were recorded using an accelerometer (Crossbow® model CXL10LP3 triaxial, range +/- 10 g) affixed to each subjects' sternum.

As this accelerometer is DC coupled, it responds to gravity and when placed on a subjects' sternum, subsequently records data in a world fixed coordinate system. Orientation of the accelerometer is rotated in the world coordinate system due to the natural backward slope of the sternum and the forward lean of a subject carrying a heavy load. The dynamic modeling software can not directly accept acceleration data and the

following strategy was developed to create a forcing function for the torso model based on human torso accelerations.

Acceleration was first converted from the recorded units of millivolts into the corresponding g values using the manufacturer supplied calibration factors for the three channels. On all three channels, recorded signals consist of two components. The first component is due to the orientation of the accelerometer in the gravitational field and the second component is due to muscle induced accelerations of the torso. Over the course of the complete circuit, the average muscle generated acceleration on any channel must be zero if the final displacement is zero. Therefore, the DC offset, which represents the average orientation of the accelerometer in the earth's gravitational field, was calculated by taking the average signal value over the circuit. This value was then subtracted from each data point leaving the component of acceleration that corresponded to muscle induced torso acceleration.

At any given moment, the orientation of the torso, and hence the accelerometer, may vary with respect to the world. VisualNastran 4D cannot solve motions described by accelerations but it is possible to prescribe an object's velocity history. Therefore, acceleration data with the DC offset due to gravity removed, was numerically integrated using the trapezoid rule to create a velocity history file. Numerical integration requires that the velocity increment due to acceleration over a time step be added to the velocity calculated at the end of the previous time step. Any error in previous velocity calculation is carried forward and accumulates. It is necessary to regularly apply known conditions to remove this accumulating error. Using the fact that when the velocity demonstrates an inflection point, the acceleration must have passed through a value of zero, acceleration can be forced to be zero at these points and the accumulating error can be reset to zero. An estimate of the error in the acceleration data is then based on the difference between the acceleration signal value and zero at these velocity inflection points. Compensation for this error is applied to the data until the velocity curve indicates the next inflection point. At this point the error estimate is recalculated and the process continues. Velocity is then recalculated based on the error corrected accelerations to provide a better estimate of the velocity history with the accelerometer drift accounted for.

A 10 second sample of torso medial/lateral (side to side) acceleration recorded during a simulated boulder hop activity appears in Figure 9. Figure 10 shows the side to side torso velocity initially calculated from these data. The signal drift has not been removed and the velocity appears to show a negative trend due to the accumulating error. Figure 11 shows the same data set with the correction for the signal drift applied. The tendency to accumulate error has been removed.

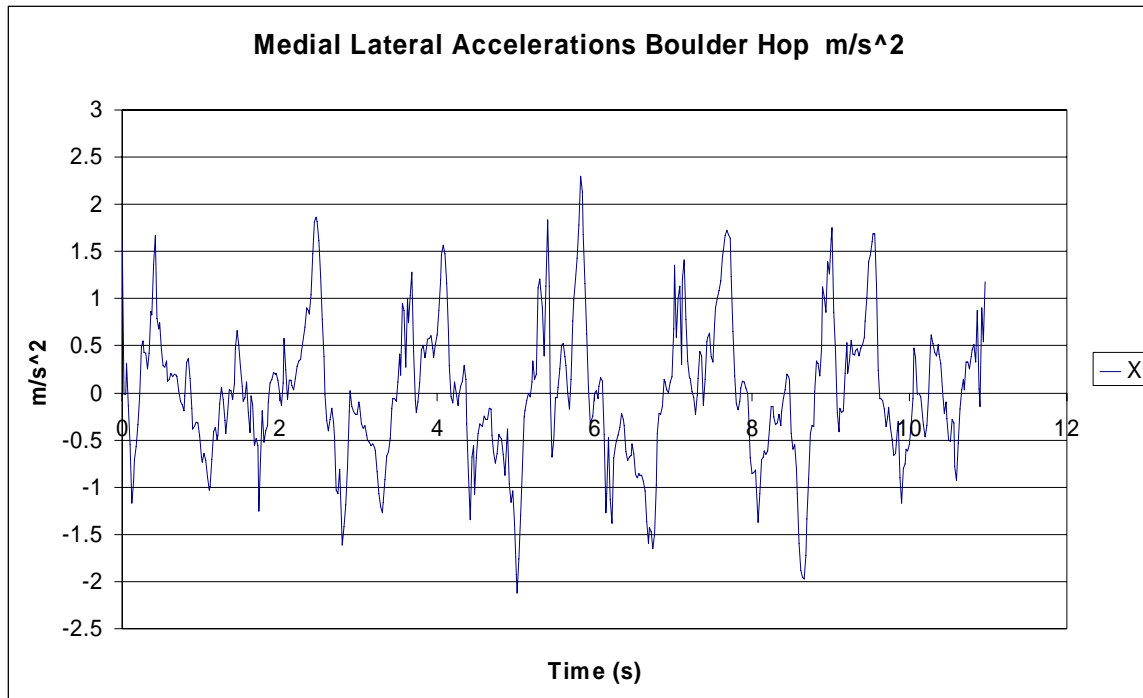


Figure 9 Medial Lateral Accelerations during Boulder Hop

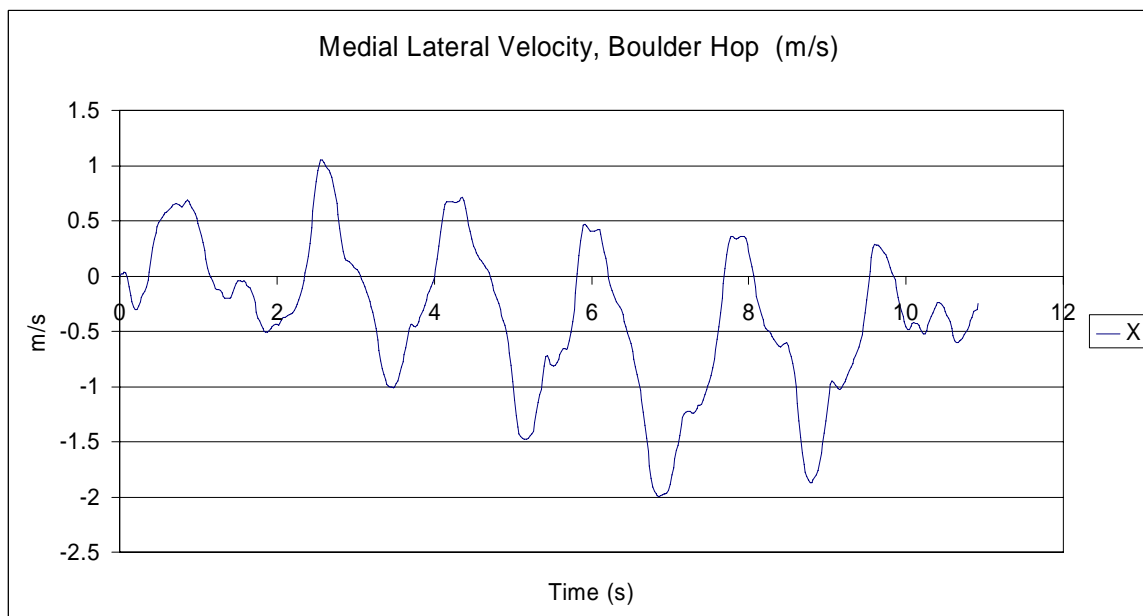


Figure 10 Medial Lateral Velocity during Boulder Hop  
No compensation for drift

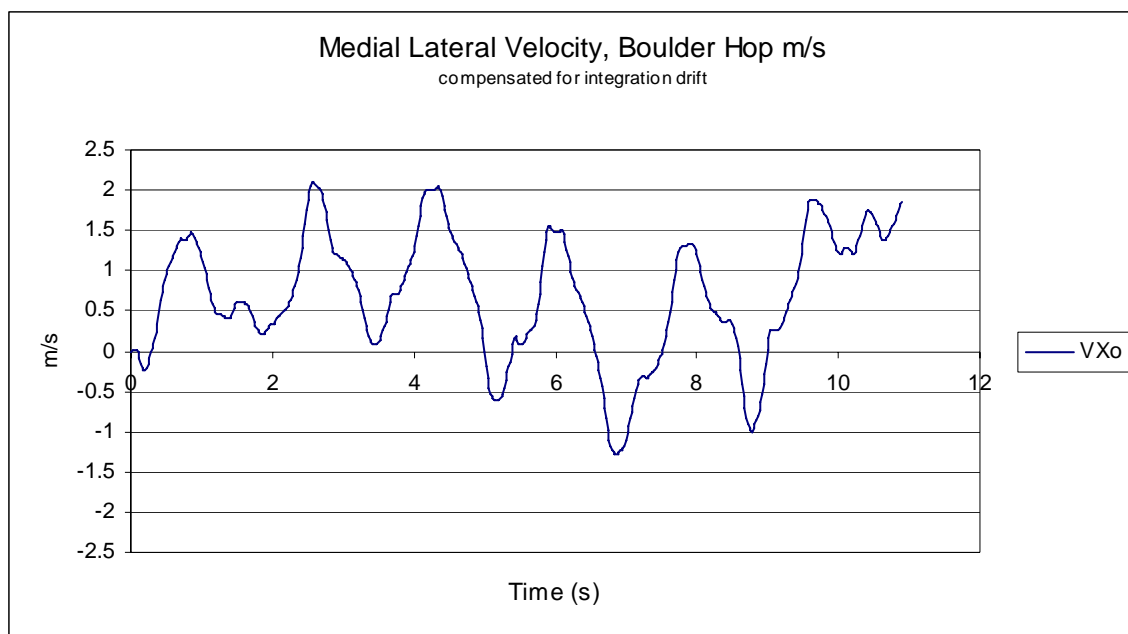


Figure 11 Error Compensated, Medial Lateral Velocity during Boulder Hop

### 4.3.1 Inputting the Forcing Function

The velocity function is input using the following steps:

1. A separate text file is created for each axis; each file containing two columns of ASCII data with no headers. Column 1 is time and column 2 is the corresponding velocity at that time.
2. The property window is opened for the accelerometer body in the model. See Figure 12.
3. The position tab is selected and “prescribed motion” chosen.
4. The appropriate ASCII text files are selected as the inputs for each axis.

Sample files from both walking and boulder hopping activities have been processed. A general Microsoft Excel® template has been created to integrate activity acceleration files and create velocity input files for the DBM.

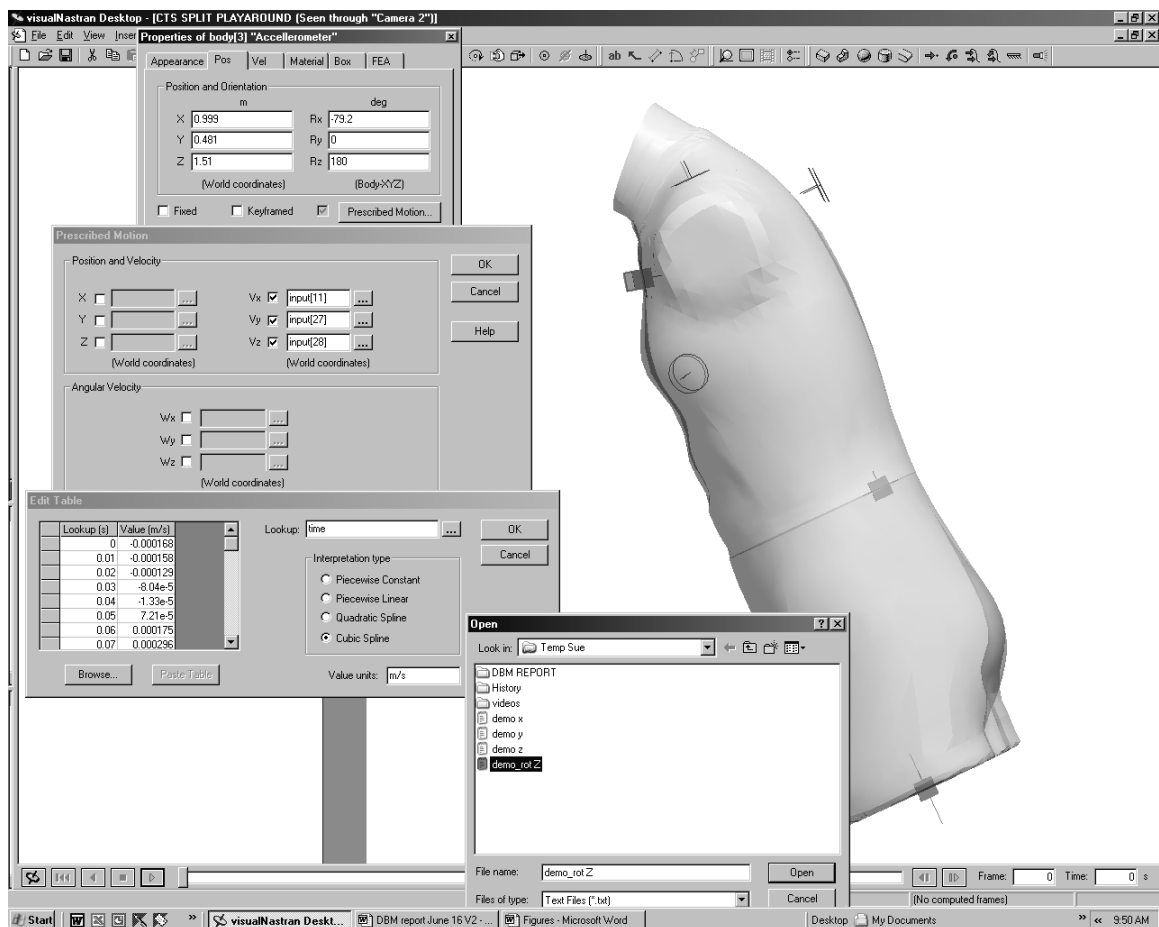


Figure 12 Creation of Prescribed Velocity Profiles

## 5.0 Model Outputs

### 5.1 Critical factor outputs

The concept of critical factor output pertains to creating analysis capabilities that evaluate known mechanisms where injury risk modes have been documented. Model output refinement will be directed at reflecting the degree of potential peril a user is experiencing given the physical demands of the mobility tasks. This concept of determining the potential injury modes and creating a model to determine the risk state of the human subject is applicable to a variety of human device interfaces.

The software permits the calculation of contact forces, displacements of bodies, forces in constraints and internal stresses using linear finite element analysis. Given a prescribed velocity profile, the model currently calculates:

- X, Y and Z contact force between the pack and the body
- Distribution of load between the upper and lower torso
- Shoulder strap forces in the upper and lower straps
- Estimated L4/L5 compression, shear and torque
- 3D displacement of the subject
- 3D displacement of the pack

For ease of visualization, a section of torso accelerations during walking was analysed and these results will be used to demonstrate model outputs. Figure 13 shows a side view of the model progressing straight forward driven by prescribed accelerometer velocities. Figure 14 shows the overhead view of the model. The X (side to side) displacement of the centre of gravity of the torso in the X-Y plane is tracked and appears on the left side of the figure immediately under the coordinate axis.

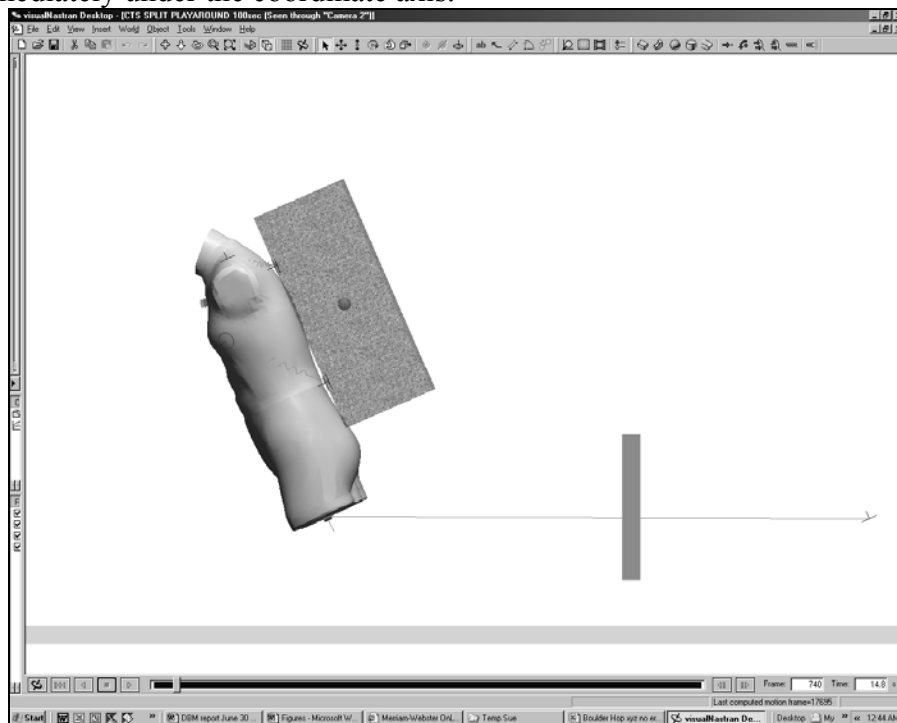


Figure 13 Side view of walking model



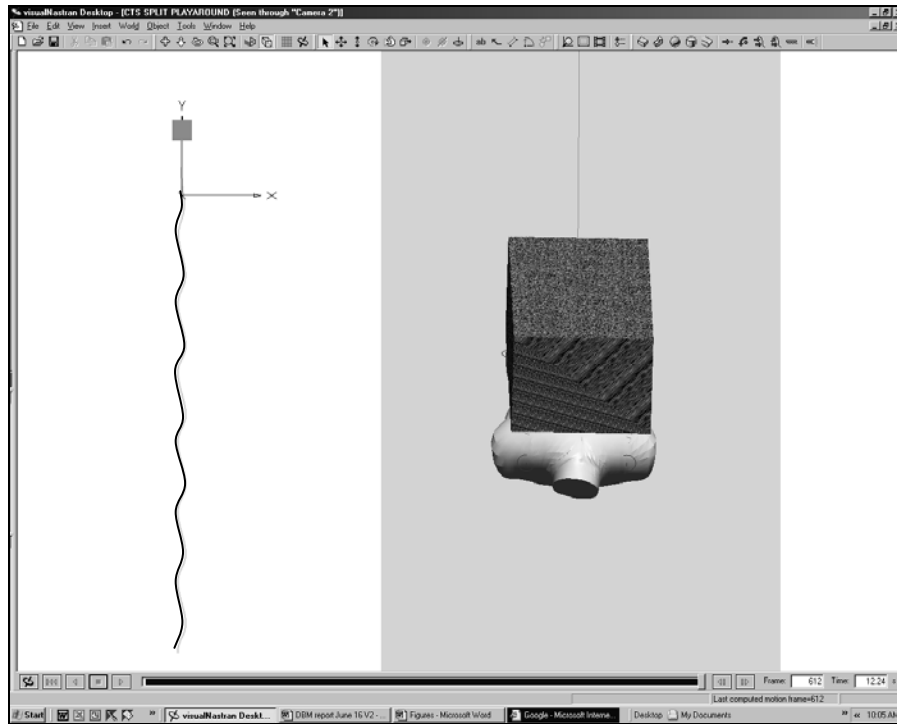


Figure 14 Plane view of walking model

## 5.2 Contact forces on body

The program outputs separate upper and lower torso contact forces and an example of the contact forces appears as Figure 15.

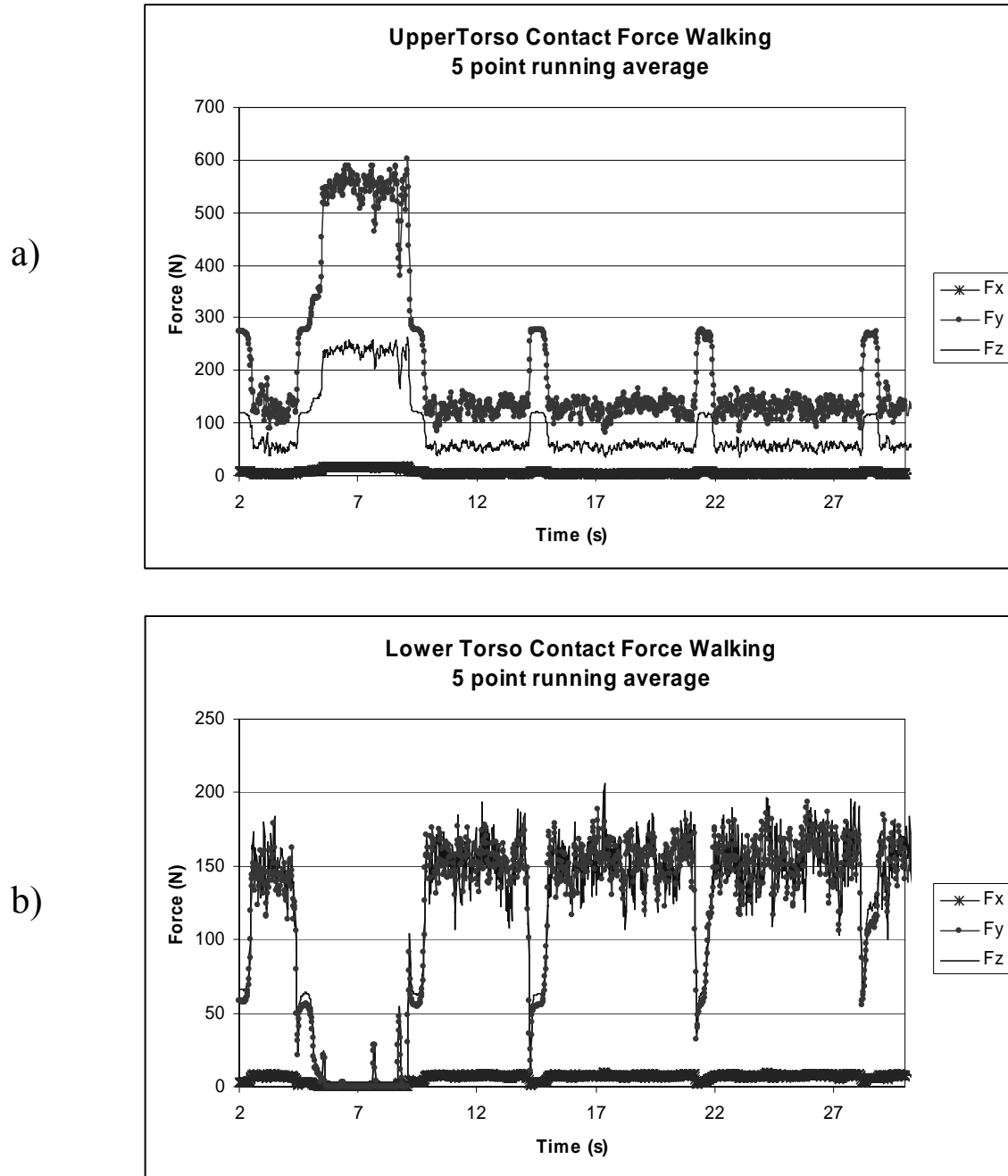


Figure 15 Contact force on torso during walking

- a) Estimated Contact force on upper torso
- b) Estimated Contact force on lower torso

## 5.3 Distribution of forces between upper and lower torso

### 5.3.1 L5/S1 shear force

In his book on low back disorders, McGill (2002) summarized a list of risk factors for low back disorders from a review of epidemiological and tissue based studies. This composite list includes “static posture...specifically prolonged trunk flexion and a twisted or laterally bent trunk” and “peak and cumulative low back shear force, compression force and extensor moment.” Static posture, trunk flexion and exposure to low back shear are typical in most backpack load carriage situations. In Figure 16, shear force is in the Y direction and vertical force is in the Z direction. The medial lateral shear in the X direction is approximately 0, indicating that the load is balanced side to side. Torques can also be plotted in the same way.

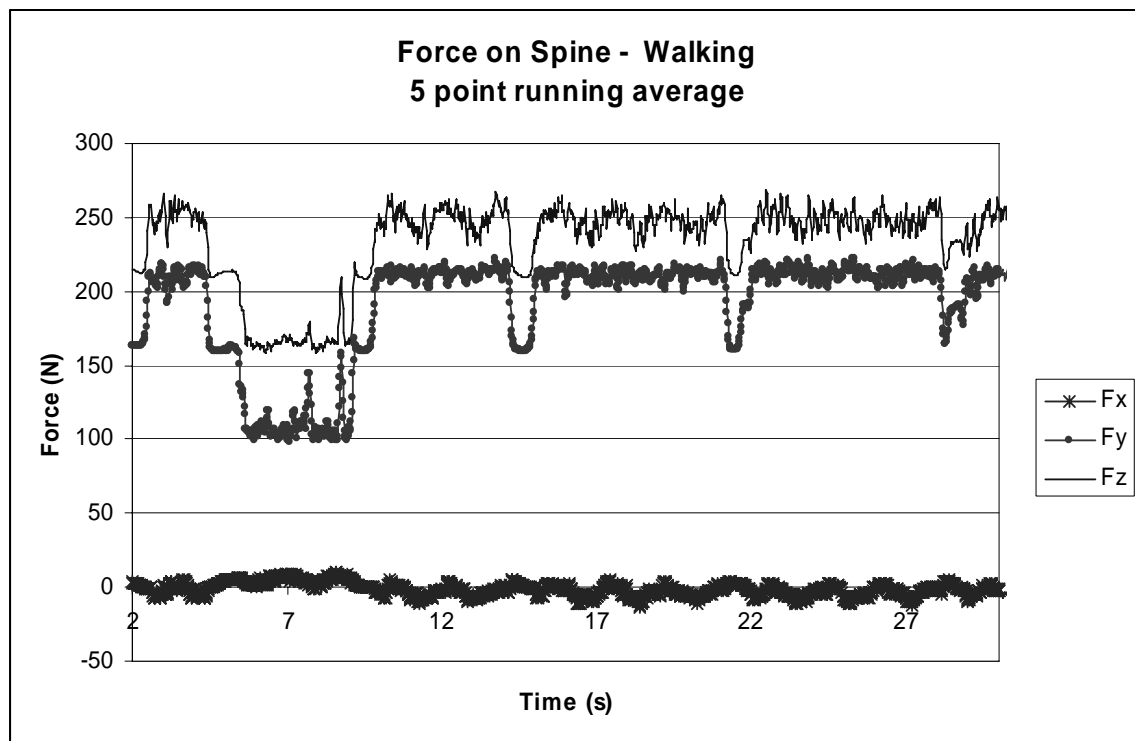


Figure 16 Estimated Forces at L5/S1

Fx = Medial/lateral Shear  
Fy = Anterior/Posterior Shear  
Fz = Vertical Compressive Load

## **6.0 Continuing Development**

Currently research is continuing to completely model all major pack components, refine the suspension system parameters and create a more automated ability to run parametric analyses of model parameters. Once the pack-person interface has been characterized, we will attempt to develop the ability to estimate contact pressure distributions on specific body regions given a set of suspension system compliance parameters. This would enable a user to take simple material property information, combine it with a component from a library of various pack parts (shoulder pads, lumbar pads or waist belt styles) and achieve a reasonable model of any backpack of interest.

### **6.1 Modeling interface contact pressures on human skin**

As any device carried on the body must distribute its weight and inertial loading through the skin and soft tissues to the skeleton, the first effect of carrying a device occurs in the body's skin layer. The DBM is not primarily a model of a load carriage system. It is also a model of a human form that determines the effect of different equipment on a set of biomechanical factors when the torso moves through a range of soldier motions.

To this end a skin layer for the torso is being developed. This layer, which ranges from 3-5 mm in thickness, will be assigned linear material properties to enable the model to estimate stresses in this layer of tissue. The tolerance of skin to contact pressure and duration pressure loading will be determined through testing and literature review.

## 7.0 References

- Bryant, JT, Doan, J, Stevenson, JM, Pelot, RP. Validation of objective based measures and development of a performance based ranking method for load carriage systems. Proceedings of the RTO – NATO Specialist Meeting, 15;1-12, 2001.
- Cholewicki, J., McGill, S.M. (1996) Mechanical stability of the in vivo lumbar spine: Implications for injury and chronic low back pain. *Clin. Biomech.* 11(1): 1-15.
- Cholewicki, J., Simons, A.P.D., and Radebold, A. (2000). Effects of external trunk loads on lumbar spine stability. *J. Biomech.* 33(11): 1377-1385.
- Marras, W.S., Lavender, S.A., Leurgans, S.E., Fathallah, F.A., Ferguson, S.A., Allread, W.G., Rajulu, S.L. (1995) Biomechanical risk factors for occupationally related low back disorders. *Ergonomics* 38: 377-410.
- McGill, S.M. *Low Back Disorders* , copyright 2002, printer Sheridan Books, USA
- McGill, S.M. (1992) A myoelectrically based dynamic three-dimensional model to predict loads on lumbar spine tissues during lateral bending. *J. Biomech.* 25: 395-414.
- McGill, S.M. (1997) The biomechanics of low back injury: Implications on current practice in industry and the clinic. *J. Biomech.* 30: 465-475.
- Naylor, P.F.D., *The skin surface and friction*, British Journal of Dermatology, 1955; V67: 238-239.
- Petit Y., Aubin C.É., Labelle H., Spinal Shape Changes Resulting from Scoliotic Spine Surgical Instrumentation Expressed as Intervertebral Rotations and Centers of Rotation, J Biomechanics, 2002 (submitted).
- Pelot, R.P., Rigby, A., Bryant, J.T., Stevenson, J.M. Section C: Phase II of a Biomechanical Model for Load Carriage Assessment. PWGSC Contract # W7711-7-7420/A (45 pgs), 1998.
- Pelot, R.P., Rigby, A., Stevenson, J.M., and Bryant, JT. Static biomechanical load carriage model. Proceedings of the RTO – NATO Specialist Meeting, 25;1-12, 2001.
- Reid, SA, Bryant, JT, Stevenson, J.M., *Phase II Development of a Dynamic Biomechanical Model of Human Load Carriage*, DRDC No. . W7711-0-7632-06, June 2002
- Sanders, J.E., Greve, J.M., Mitchell, S.B, Zachariah, S.G., *Material Properties of commonly used interface properties amd their static coefficients of friction with skin and socks*. Journal of Rehabilitation Research and Development, Jn 1998, V35, No.2: 161-176.

Stevenson, JM, Bryant, JT, Reid, SA, Pelot, RP, Morin EL *Development of the Canadian Integrated Load Carriage System using Objective Measures*. Proceedings of the RTO – NATO Specialist Meeting, 21;1-11, 2001.

Stevenson, JM, Reid, SA, Bryant, JT, Hadcock, L.J., Morin, EL *Part A of Phase I: Equipment Upgrades to Accommodate Dynamic Biomechanical Modeling* subsection of: *Development of a Dynamic Biomechanical Model for Load Carriage: Phase I* PWGSC Contract # W7711-0-7632-01/A, March 2001

Stevenson, JM, Good, J.A. Devenney, I.A. *Characterization of Load Control During a Human Trials Circuit Phase 3(b)*, DRDC No. W7711-0-7632-06, June 2002

Stevenson, JM, Bryant JT, Reid, SA, Pelot, RP, Morin, EL, Bossi LL. Development and Assessment of the Canadian personal load carriage system using objective biomechanical measures. (Accepted with revisions: Ergonomics, April 2003).

## **Technical Reports**

Stevenson, J.M., Bryant, J.T., Reid, S.A. and Pelot, R.P. Validation of the Load Carriage Simulator: Research and Development of an Advanced Personal Load Carriage system: Section D (Phase 1). DSS Contract #W7711-4-7225/01 (44 pgs). 1996

Stevenson, J.M., Bryant, J.T., dePencier, R.D., Pelot, R.P., and Reid, J.G. Research and Development of an Advanced Personal Load Carriage System (Phase I-D). DSS Contract # W7711-4-7225/01-XSE (350 pgs). 1995

## **Appendix A - Compression Testing of Five Foam Materials**

Author: Leone Pleog,<sup>1</sup> MSc. P.Eng.  
April 2, 2003

<sup>1</sup>Human Mobility Research Centre  
Syl and Molly Apps Research Centre  
Kingston General Hospital  
Kingston On K7L 2V7  
(613) 549-2529

## Scope

This Appendix describes the test set-up and the results obtained testing 5 foam specimens in the Instron Material Testing System.

### A1) Test Description

#### A1.1) Test Equipment

An Instron material testing machine was used with a 500kg Load cell. The indenter was a cylindrical fixture with a flat contact surface area of  $25.9 \text{ cm}^2$ . It was connected to the crosshead of the Instron. A cylinder measuring 6.2 cm high and 15.2 cm in diameter was bolted to the base of the Instron. Figure A-1 is a photo of the Instron with a specimen ready for testing. Instron Merlin Software was used to run the test and collect the data.

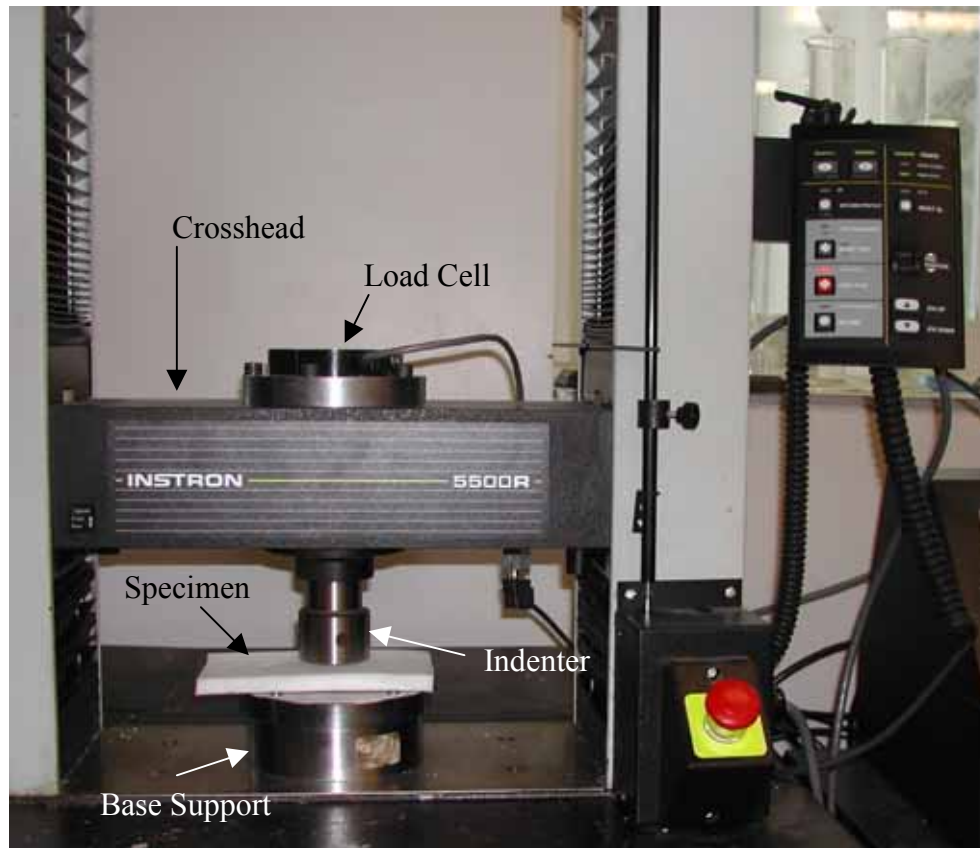


Figure A-1: Material Testing System



### A1.2) Test Samples

4 pieces of foam (Figure A-2) and a backpack strap were tested.



Figure A-2: Foam specimens

### A1.3) Test Loading Patterns

#### A1.3.1) Dynamic testing

For the dynamic testing the Instron Merlin Software was programmed to ramp up to a pressure of 60 kPa over 30 seconds, hold for 10 seconds, then perform a cyclic ramp  $\pm 20$  kPa for 60 seconds. The first trial used a cyclic ramp of 1.8 Hz and the second 3.5 Hz. Figure A-3 is a screen capture of the profile programmed in the Instron Merlin Software

#### A1.3.2) Creep Testing

For creep testing the load pattern was a slow ramp (30 seconds) followed by a hold for 300 seconds. This was repeated for 3 different pressures: 20 kPa, 40 kPa and 60 kPa. Figure A-4 is a screen capture of the profile programmed in the Instron Merlin Software.

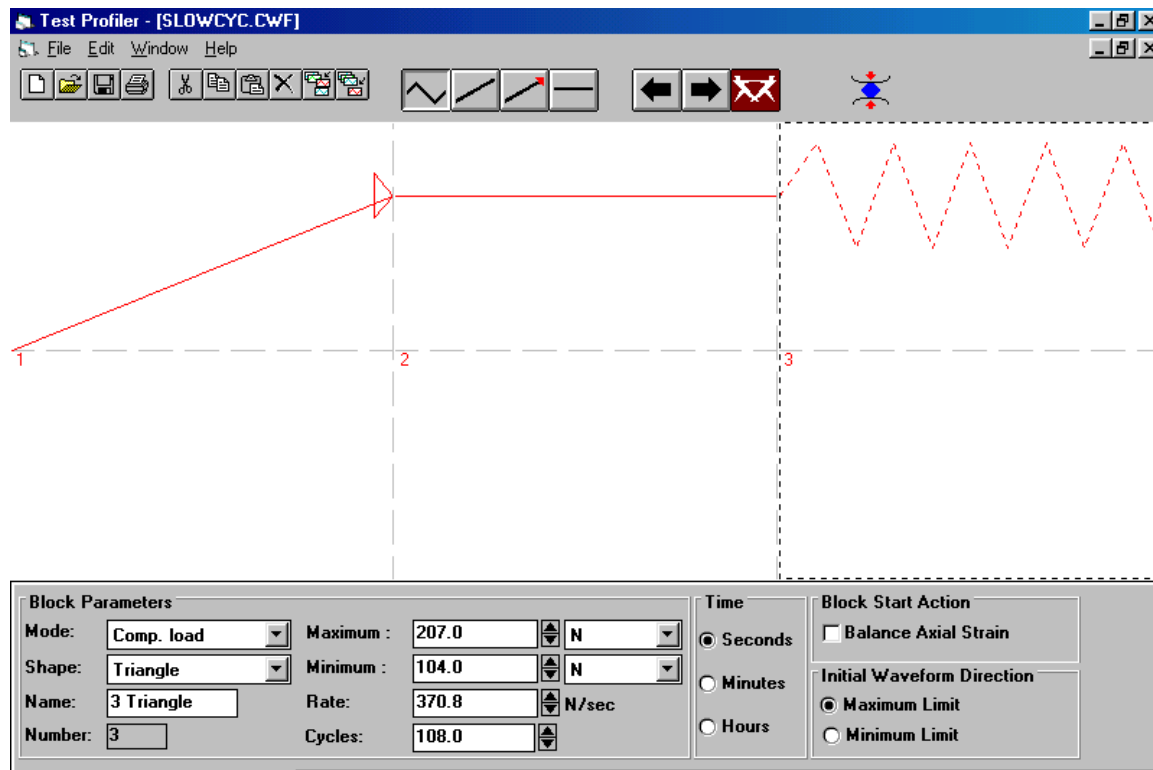


Figure A-3: Test Profile for Dynamic tests

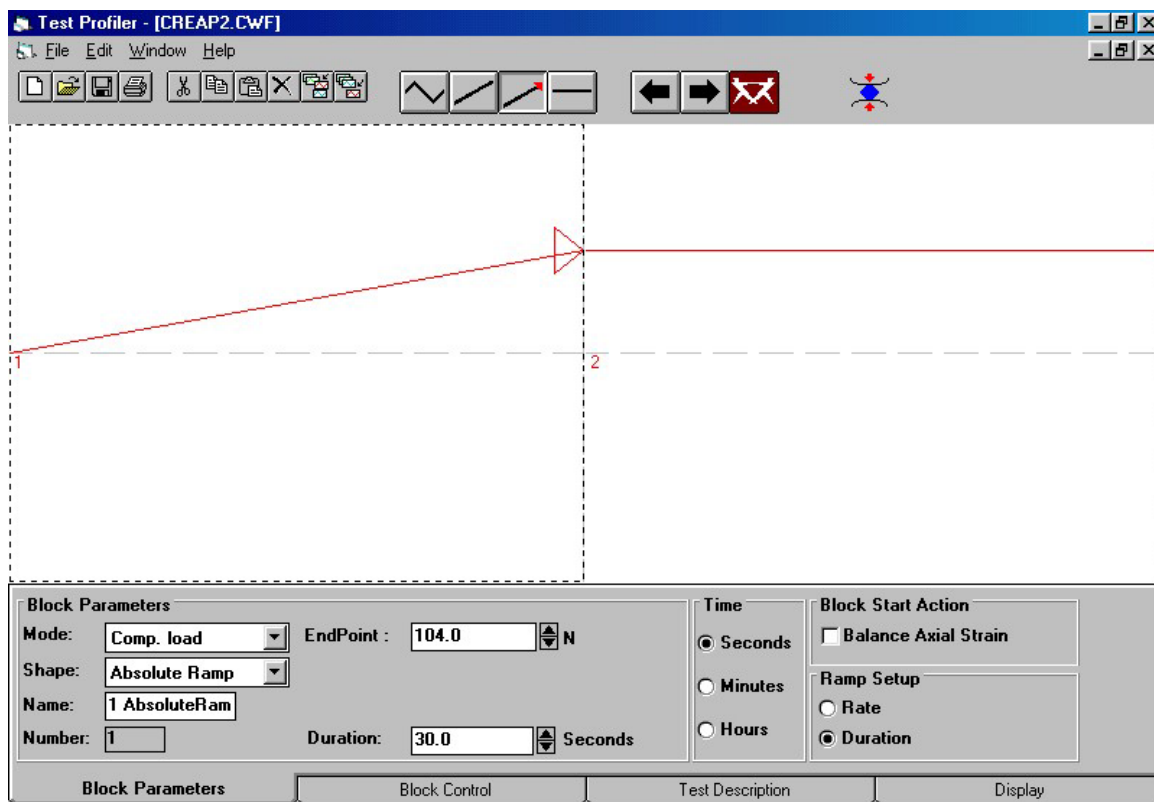


Figure A-4: Test Profile for Creep tests

## A1.4) Test Methods

The Instron was programmed with the appropriate profile. The indenter was raised the thickness of the test sample from the base support. The test sample was placed on the base plate and the test initiated.

Between each test, the specimen was given a recovery time of at least twice the duration of the test. Where possible the specimen was moved between tests such that different sections were tested.

Each test was repeated three times for each specimen except for the higher frequency dynamic test.

## A2) Test Results

### A2.1) Dynamic Testing

#### A2.1.1) Cyclic Frequency of 1.8 Hz

The Instron was unable to produce 1.8 Hz with any of the samples. Only the Trocellan, EVA and Ether sample were close to the desired pressure ranges. These results are summarized in Table A-1.

Sample	Min Load (kPa)	Max Load (kPa)	Freq (Hz)
Target values	40	80	1.8
Trocellan	39.6	80.5	1.5
Volara	24.7	107.7	1.4
EVA	40.0	85.0	0.66
Ether	34.7	85.4	1.5
Strap	19.5	146.5	1.0

Table A-1: Target versus actual results

Trocellan underwent the least amount of deflection and the backpack strap the most. However, it should be taken into consideration that the tests were not all within the same pressure ranges. Table A-2 lists the samples in order of deflection.

Sample	Min-Max Deflection (mm)	Sample Thickness (mm)
Trocellan	1.0-1.2	6.3
Volara	1.3-2.9	5.8
EVA	3.1-5.3	14.1
Ether	8.5-9.0	10.9
Strap	11.0-16.0	26.1

Table A-2: Deflection Range for cycling at 1.8 Hz

The slope of the initial unloading on the stress strain-curves was calculated for one cycle of each sample. These results are summarized in Table A-3.

<b>Sample</b>	<b>Young's Modulus (kPa)</b>
EVA	378.6
Volara	398.5
Strap	2720.3
Trocellan	3287.3
Ether	4204.5

Table A-3: Young's Modulus for each sample

## A2.2) Dynamic Testing

### A2.2.1) Cyclic Frequency of 3.5 Hz

The Instron was unable to produce 3.5 Hz with any of the samples. Trocellan, was the closest to the desired pressure ranges. None were within the desired pressure range. These results are summarized in Table A-4.

<b>Sample</b>	<b>Min Load (kPa)</b>	<b>Max Load (kPa)</b>	<b>Freq (Hz)</b>
Target values	40	80	3.5
Trocellan	33.9	86.4	2.3
Volara	13.3	158.3	1.5
EVA	1.8	246.0	1.0
Ether	29.1	98.4	2.2
Strap	8.6	249.6	1.1

Table A-4: Target versus actual results

Trocellan underwent the least amount of deflection and the backpack strap the most. However, it should be taken into consideration that the tests were not all within the same pressure ranges. Table A-5 lists the samples in order of deflection.

<b>Sample</b>	<b>Min-Max Deflection (mm)</b>	<b>Sample Thickness (mm)</b>
Trocellan	0.4-0.6	6.3
Volara	1.3-2.9	5.8
EVA	3.1-5.3	14.1
Ether	8.5-9.0	10.9
Strap	11.0-16.0	26.1

Table A-5: Deflection Range for cycling at 3.5 Hz

The slope of the initial unloading on the stress strain-curves was calculated for one cycle of each sample. These results are summarized in Table A-6.

<b>Sample</b>	<b>Young's Modulus (kPa)</b>
EVA	14769.8
Volara	-1014.0
Strap	-45571.8
Trocellan	3500.0
Ether	16918.3

Table A-6: Young's Modulus for each sample

### A2.3) Creep Testing

Table A-7 lists the slopes of the various displacement versus time curves for the section of the curve after 100 seconds had elapsed.

<b>Sample</b>	<b>Slope of Displ vs Time curve at specified Load</b>		
	<b>20 kPa</b>	<b>40 kPa</b>	<b>60 kPa</b>
Trocellan	0.00004	0.00006	0.0001
Volara	0.00008	0.0001	0.0001
Eva	0.0003	0.0007	0.0007
Ether	0.0007	0.0003	0.0002
Strap	0.001	0.0008	0.0008

Table A-7: Slope of displacement versus time c



## Appendix B - Calculation of Torso lean from acceleration

If the accelerometer axes mounted on the torso were exactly aligned with a global right hand coordinate system, all the acceleration due to gravity would appear only on the -X axis. However, the sternum is not typically aligned with  $X_g$  and so the initial orientation of the accelerometer must be calculated.

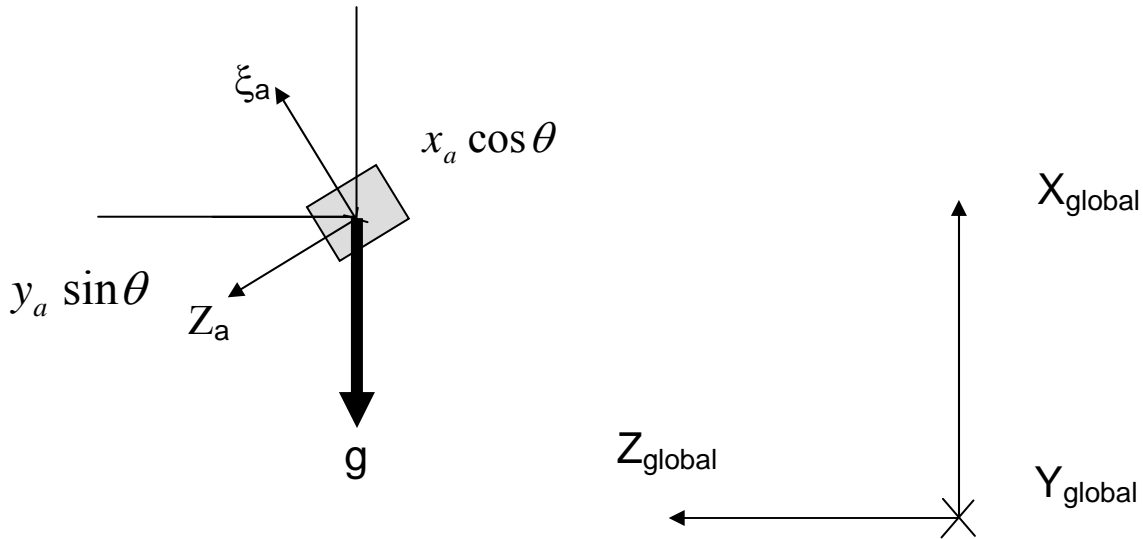


Figure B-1: Accelerometer Orientation in the Earth's Gravitational Field

The solution for  $\theta$  is :

$$x_a \cos \theta - y_a \sin \theta - g = 0 \quad \text{Equation 1}$$

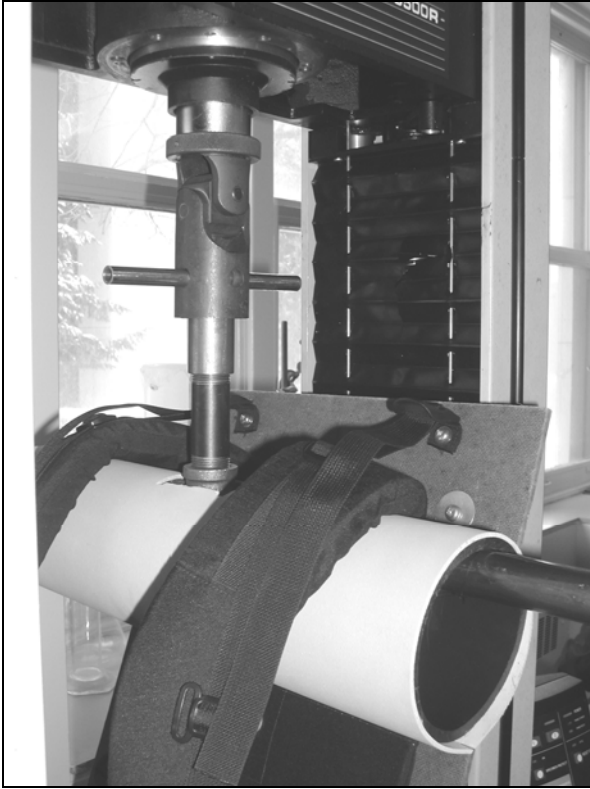
Equation 1 must be solved by iteration.

A baseline orientation of the accelerometer can be calculated from an initial standing posture.



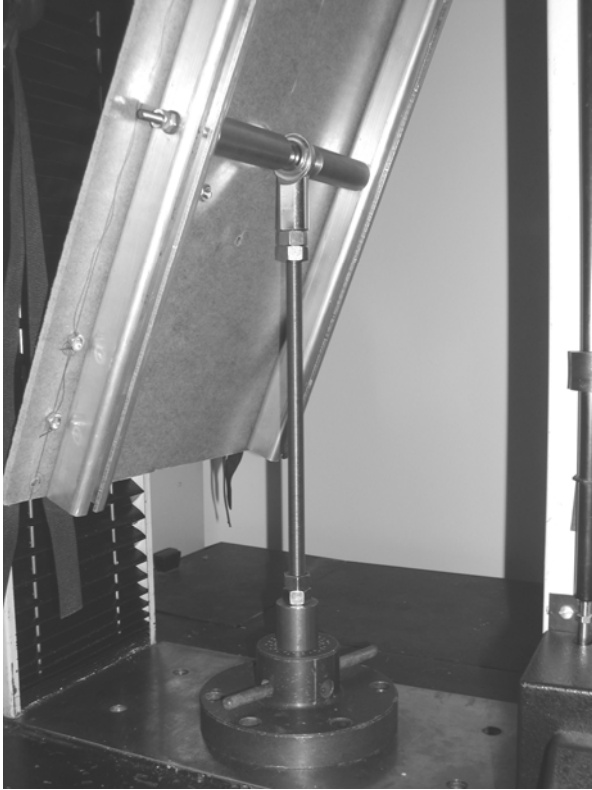


## Appendix C - Details of the Suspension Testing Jig



The universal joint and the clevis style attachment to the “shoulder” section of the apparatus ensures pure tension on the suspension system. The yoke and straps were held in the correct relative positions and bolted to a rigid fibreboard frame

Figure C-1 Detail of Upper Attachment.



The rod end connection allows 180 degree rotation about the attachment axis and  $\pm 13$  degree rotation medial/laterally to permit the apparatus to self align. Care was taken to ensure that the applied load did not induce any bending moment and the Instron Universal testing machine applied pure tension to the suspension system. The lower attachment is rigidly fixed to the Instron frame.

Figure C-2 Detail of Lower Attachment



When assembled, the shoulder and load lifter straps were tightened to a marked, preset length. These lengths had been measured from a human worn CTS pack.

Figure C-3 Suspension Tester

# UNCLASSIFIED

<b>DOCUMENT CONTROL DATA</b> (Security classification of the title, body of abstract and indexing annotation must be entered when the overall document is classified)		
<b>1. ORIGINATOR</b> (The name and address of the organization preparing the document, Organizations for whom the document was prepared, e.g. Centre sponsoring a contractor's document, or tasking agency, are entered in section 8.)  Publishing: DRDC Toronto Performing: Ergonomics Research Group – Human Mobility Research Centre, Queen's University, Kingston, Ontario K7L 3N6 Monitoring: Contracting: DRDC Toronto		<b>2. SECURITY CLASSIFICATION</b> (Overall security classification of the document including special warning terms if applicable.)  <b>UNCLASSIFIED</b>
<b>3. TITLE</b> (The complete document title as indicated on the title page. Its classification is indicated by the appropriate abbreviation (S, C, R, or U) in parenthesis at the end of the title)  <b>Development of a Dynamic Biomechanical Model for Load Carriage: Phase IV Part A</b> <b>Development of a Dynamic Biomechanical Model Version 2 of Human Load Carriage (U)</b>		
<b>4. AUTHORS</b> (First name, middle initial and last name. If military, show rank, e.g. Maj. John E. Doe.)  <b>S.A. Reid; J.T. Bryant; J.M. Stevenson; M. Abdoli</b>		
<b>5. DATE OF PUBLICATION</b> (Month and year of publication of document.)  <b>August 2005</b>	<b>6a NO. OF PAGES</b> (Total containing information, including Annexes, Appendices, etc.)  <b>53</b>	<b>6b. NO. OF REFS</b> (Total cited in document.)  <b>19</b>
<b>7. DESCRIPTIVE NOTES</b> (The category of the document, e.g. technical report, technical note or memorandum. If appropriate, enter the type of document, e.g. interim, progress, summary, annual or final. Give the inclusive dates when a specific reporting period is covered.)  <b>Contract Report</b>		
<b>8. SPONSORING ACTIVITY</b> (The names of the department project office or laboratory sponsoring the research and development – include address.)  Sponsoring: Tasking:		
<b>9a. PROJECT OR GRANT NO.</b> (If appropriate, the applicable research and development project or grant under which the document was written. Please specify whether project or grant.)  <b>12CM03</b>		<b>9b. CONTRACT NO.</b> (If appropriate, the applicable number under which the document was written.)  <b>W7711-0-7632-07</b>
<b>10a. ORIGINATOR'S DOCUMENT NUMBER</b> (The official document number by which the document is identified by the originating activity. This number must be unique to this document)  <b>DRDC Toronto CR 2005-123</b>		<b>10b. OTHER DOCUMENT NO(s).</b> (Any other numbers under which may be assigned this document either by the originator or by the sponsor.)
<b>11. DOCUMENT AVAILABILITY</b> (Any limitations on the dissemination of the document, other than those imposed by security classification.)  <b>Unlimited distribution</b>		
<b>12. DOCUMENT ANNOUNCEMENT</b> (Any limitation to the bibliographic announcement of this document. This will normally correspond to the Document Availability (11). However, when further distribution (beyond the audience specified in (11) is possible, a wider announcement audience may be selected.))  <b>Unlimited announcement</b>		

**UNCLASSIFIED**

## **UNCLASSIFIED**

### **DOCUMENT CONTROL DATA**

(Security classification of the title, body of abstract and indexing annotation must be entered when the overall document is classified)

13. **ABSTRACT** (A brief and factual summary of the document. It may also appear elsewhere in the body of the document itself. It is highly desirable that the abstract of classified documents be unclassified. Each paragraph of the abstract shall begin with an indication of the security classification of the information in the paragraph (unless the document itself is unclassified) represented as (S), (C), (R), or (U). It is not necessary to include here abstracts in both official languages unless the text is bilingual.)

(U) The purpose of this DRDC dynamic biomechanical model research program is to improve the understanding of human load carriage capabilities and to understand the effects of load carriage design features on human health and mobility. This research is directed at creating a method of determining several of the biomechanical factors to be used as inputs to the Load Conditions Limit model as described in DRDC report # W7711—0—7632—01 entitled “Proposed Long Range Plan for a Research and Development Program of Dynamic Load Carriage Modeling”

In the current study, a 3D solid model was split into an upper and lower torso coupled with a rigid join located at the location of the spine at the L3/L2 height. Acceleration histories of subjects wearing packs were previously recorded during human trials (Morin et al, 2002). Acceleration of a person was numerically integrated and used to drive the motion of the Dynamic Biomechanical Model (DBM) torso. Torso accelerations for a wide range of activities were recorded and can be used to drive these models, creating an excellent data base for many human and pack motions for current and future modeling of human motions. This technique of capturing and generating motions is applicable to many situations where an envelope of human motion and body accelerations needs to be tested to ensure equipment does not cause excessive dynamic loading on the soldier. Piecewise linear dynamic, static and creep material response models were developed for typical backpack materials. In addition, a piecewise linear model of the dynamic stress-strain response for the Cloth the Soldier shoulder strap assembly was developed. The model estimates reaction forces and moments on the lumbar spine and the total shoulder reaction force. The model also calculates the distribution of force to the upper and lower torso and the total contact force.

Work is proceeding on incorporating a skin layer and creating the ability to examine interaction details at the equipment – skin interface. The final goal is to estimate injury risk potential across a range of activities and loads.

14. **KEYWORDS, DESCRIPTORS or IDENTIFIERS** (Technically meaningful terms or short phrases that characterize a document and could be helpful in cataloguing the document. They should be selected so that no security classification is required. Identifiers, such as equipment model designation, trade name, military project code name, geographic location may also be included. If possible keywords should be selected from a published thesaurus, e.g. Thesaurus of Engineering and Scientific Terms (TEST) and that thesaurus identified. If it is not possible to select indexing terms which are Unclassified, the classification of each should be indicated as with the title.)

(U) Load carriage; Dynamic Biomechanical Model; 3D Model; CTS Pack; Suspension System; Force Distribution; Contact Pressures; Modeling Interface

**UNCLASSIFIED**